

Refining the eruptive history of Ulleungdo and Changbaishan volcanoes (East Asia) over the last 86 kyrs using distal sedimentary records

Article

Accepted Version

Creative Commons: Attribution-Noncommercial-No Derivative Works 4.0

McLean, D., Albert, P. G., Suzuki, T., Nakagawa, T., Kimura, J.-I., Chang, Q. C., MacLeod, A., Blockley, S., Staff, R. A., Yamada, K., Kitaba, I., Haraguchi, T., Kitagawa, J., SG14 Project Members, and Smith, V. C. (2020) Refining the eruptive history of Ulleungdo and Changbaishan volcanoes (East Asia) over the last 86 kyrs using distal sedimentary records. *Journal of Volcanology and Geothermal Research*, 389. 106669. ISSN 0377-0273 doi: <https://doi.org/10.1016/j.jvolgeores.2019.106669> Available at <https://centaur.reading.ac.uk/86408/>

It is advisable to refer to the publisher's version if you intend to cite from the work. See [Guidance on citing](#).

To link to this article DOI: <http://dx.doi.org/10.1016/j.jvolgeores.2019.106669>

Publisher: Elsevier

All outputs in CentAUR are protected by Intellectual Property Rights law, including copyright law. Copyright and IPR is retained by the creators or other

copyright holders. Terms and conditions for use of this material are defined in the [End User Agreement](#).

www.reading.ac.uk/centaur

CentAUR

Central Archive at the University of Reading

Reading's research outputs online

REFINING THE ERUPTIVE HISTORY OF ULLEUNGDO AND CHANGBAISHAN VOLCANOES (EAST ASIA) OVER THE LAST 86 KYRS USING DISTAL SEDIMENTARY RECORDS

DANIELLE MCLEAN^{*a}, PAUL G ALBERT^a, TAKEHIKO SUZUKI^b, TAKESHI NAKAGAWA^c, JUN-ICHI KIMURA^d, QING CHANG^d, ALISON MACLEOD^{e,f}, SIMON BLOCKLEY^e, RICHARD A STAFF^{a,g}, KEITARO YAMADA^c, IKUKO KITABA^c, TSUYOSHI HARAGUCHI^h, JUNKO KITAGAWAⁱ, SG14 PROJECT MEMBERS^j AND VICTORIA C SMITH^a

^a *Research Laboratory for Archaeology and the History of Art, University of Oxford, Oxford, OX1 3TG, UK*

^b *Department of Geography, Tokyo Metropolitan University, Tokyo, 192-0397, Japan*

^c *Research Centre for Palaeoclimatology, Ritsumeikan University, Shiga, 525-8577, Japan*

^d *Department of Solid Earth Geochemistry, Japan Agency for Marine-Earth Science and Technology, Yokosuka, Japan*

^e *Department of Geography, Royal Holloway University of London, TW20 OEX, UK*

^f *Department of Geography and Environmental Science, University of Reading, RG66AB, UK*

^g *Scottish Universities Environmental Research Centre, University of Glasgow, East Kilbride, G75 0QF, UK*

^h *Osaka City University, Osaka, 558-8585, Japan*

ⁱ *Fukui Prefectural Satoyama-Satoumi Research Institute, Wakasa, 919-1331 Japan*

^j *www.suigetsu.org*

**Corresponding author: mclean.tephra@gmail.com*

Highlights:

- Distal records show eruptions are more frequent and widespread
- At least 8 Changbaishan eruptions produced widespread ash over the last 86 kyrs
- Explosive eruption of Changbaishan at ca. 42.5 ka dispersed ash >1000 km

- 4 Ulleungdo eruptions are now precisely dated using the Lake Suigetsu chronology
- U-Ym tephra is identified in Suigetsu and dated to 40,332 – 39,816 IntCal13 yrs BP

Abstract

The eruptive histories of Ulleungdo (South Korea) and Changbaishan (North Korea/China border) volcanoes are not well constrained since their proximal stratigraphies are poorly exposed or largely inaccessible. However, determining the past behaviour of these volcanoes is critical since future eruptions are likely to disperse ash over some of the world's largest metropolitan regions. Alkaline tephra deposits erupted from both centres are routinely identified in marine cores extracted from the Sea of Japan, as well as high-resolution lacustrine records east of the volcanoes. Here, we review the distal ash occurrences derived from Ulleungdo and Changbaishan and provide new data from the Lake Suigetsu (central Honshu, Japan) sediment core, in order to provide a more complete and constrained eruption framework. The intensely-dated Lake Suigetsu archive provides one of the most comprehensive distal eruption records for both centres, despite being located ca. 500 km E of Ulleungdo and ca. 1000 km SSE of Changbaishan. The Suigetsu record is utilised to precisely date and geochemically fingerprint (using major, minor and trace element glass compositions) ash fall events that reached central Honshu. Here, we identify a new non-visible (cryptotephra) layer in the Suigetsu sediments, which reveals a previously unreported explosive event from Changbaishan at 42,750 – 42,323 IntCal13 yrs BP (95.4 % confidence interval). This event is chronologically and

geochemically distinct from the B-J (Baegdusan-Japan Basin) tephra reported in the Sea of Japan (ca. 50 ka). Furthermore, we also confirm that the widespread U-Ym tephra erupted from Ulleungdo reached central Japan, and is herein dated to 40,332 – 39,816 IntCal13 yrs BP (95.4 % confidence interval). This terrestrial ¹⁴C-derived age of the U-Ym can be used to constrain the chronology of marine records containing the same marker layer. This reviewed and integrated tephrostratigraphic framework highlights the pivotal role that distal sedimentary records can play in evaluating the eruptive histories and hazard potential of Ulleungdo and Changbaishan.

Keywords: Ulleungdo, Changbaishan; Glass geochemistry; Eruption history; Sedimentary archives; Lake Suigetsu

1. Introduction

Intraplate volcanoes Ulleungdo (South Korea) and Changbaishan (North Korea/China border) are responsible for two of the largest Holocene eruptions (\geq Volcanic Explosivity Index (VEI) 6; Newhall and Self, 1982) in East Asia, blanketing large parts of Japan and the surrounding seas in ash (Figure 1; Machida and Arai, 2003). Fine ash from the AD 946 ‘Millennium Eruption’ (ME) (Hakozaki et al., 2017; Oppenheimer et al., 2017) of Changbaishan has also been identified ca. 9000 km from its source in northern Greenland (Sun et al., 2014a), which demonstrates the enormous potential of the volcano to cause major disruption to airspace across the East Asian and Pacific region. Yet, the complete eruptive histories of Ulleungdo and Changbaishan are not well

constrained since proximal eruption deposits are poorly exposed and are largely inaccessible.



Figure 1. (a) Location of Ulleungdo (South Korea; blue triangle) and Changbaishan (North Korea/China; orange triangle) and other sources of Japanese tephras outlined in the text (black triangles). Distal sites mentioned in the text are marked by white circles; 1 = Marine cores; Lim et al. (2013); 2 = Marine cores; Arai et al. (1981); Chun et al. (2007); 3 = Marine cores; Chun et al. (2007); 4 = Lake Biwa; Nagahashi et al. (2004); 5 = Marine cores; Ikehera et al. (2004); 6 = Yuanchi Lake; Sun et al. (2018); 7 = Marine cores; Ikehara (2003); 8 = Lake Hane; Sawada et al. (1997); 9 = Marine cores; Derkachev et al. (in press); 10 = Hakusan volcano; Higashino et al. (2005); 11 = Lake Kushu; Chen et al. (2016, 2019). A white star notates the location of Lake Suigetsu, and ocean basins are marked in grey (JB= Japan Basin; YR= Yamato Rise; OR= Oki Ridge; UB = Ulleungdo Basin). Dispersal boundaries of the B-Tm (AD 946; Oppenheimer et al., 2017), U-Oki (ca. 10 ka) and U-Ym (ca. 40 ka) are marked by dashed lines (B-Tm and U-Oki as defined by Machida and Arai, 2003). (b) Location of Lake Suigetsu, which is the largest of the five Mikata lakes, adjacent to Wakasa Bay. The positions of coring campaigns SG06 and SG14 are marked on Lake Suigetsu (modified after Nakagawa et al., 2005).

It is likely that proximal evidence of older eruptions, especially those of low- to mid-intensity, have been destroyed, or are now completely buried, following more recent large magnitude Holocene events. At Changbaishan clear depositional breaks and soil horizons are not well documented within proximal eruption successions (e.g., Chen et al., 2016; Sun et al., 2017), making it unclear how many eruption deposits are preserved.

Distal sedimentary records (e.g., marine and lacustrine sequences) have proved very important archives of past explosive eruptions, and can be used to help constrain the frequency and dispersal of tephra-forming events (e.g., Wulf et al., 2004; Albert et al., 2013; 2018; Smith et al., 2013; Tomlinson et al., 2014; Ponomareva et al., 2018). Ulleungdo and Changbaishan are the only sources known to have dispersed alkaline tephra across Japan (Machida and Arai, 2003; Kimura et al., 2015; Albert et al., 2019), and their distal deposits can be easily discriminated from other intraplate sources in the back-arc (e.g., Doki and Jeju volcanoes; Brenna et al., 2014). Tephra layers preserved in marine cores extracted from the Sea of Japan (Oki ridge, Yamato and Japan basins; Figure 1), indicate that both Ulleungdo and Changbaishan have been very active during the Late Quaternary, however the number and precise timing of these events remains uncertain. This is partly since successive eruption deposits are difficult to geochemically distinguish, and because marine cores in some localities are susceptible to reworking processes (e.g., turbidites; Albert et al., 2012; Cassidy et al., 2014), and often cannot be precisely dated (i.e., due to variations in the marine radiocarbon reservoir; Ikehara et al., 2013).

In order to provide new insight into the eruptive histories of Ulleungdo and Changbaishan, this study provides a detailed review of the distal occurrences of alkaline ash deposited in sedimentary records (marine and lacustrine cores) spanning the last 86 kyrs (i.e., post-dating the widespread Aso-4 tephra that is dated to 86.4 ± 1.1 ka using the $^{40}\text{Ar}/^{39}\text{Ar}$ method; Albert et al., 2019). We also provide new tephra data from the intensely-dated Lake Suigetsu archive (central Honshu, Japan), a record that has significant potential to develop a comprehensive eruption history for both centres (despite being located 500 km E of Ulleungdo and 1000 km SSE of Changbaishan). Using the lake sediments, we identify and geochemically characterise two new ash layers erupted from Ulleungdo and Changbaishan, allowing these eruptive events to be precisely dated for the first time. New trace element data are also generated for the previously identified marker layers preserved as cryptotephra in the Holocene sediments (McLean et al., 2018), offering new possibilities to discriminate between successive eruption deposits. This reviewed and integrated distal eruption framework for Ulleungdo and Changbaishan permits critical new insight into the hazard potential of these active centres.

2. Regional setting and proximal volcanic deposits

2.1. Ulleungdo Island, South Korea

Ulleungdo Island (12 km x 10 km) is the sub-aerial portion of a Quaternary stratovolcano located in the mid-western part of the Sea of Japan (37°30'N, 130°52'E), 130 km east of the Korean Peninsula (Figure 1; Kim, 1985).

Ulleungdo is the youngest volcano in the back-arc basin, and is known to have erupted intermittently from the Pliocene until the mid-Holocene (Kim et al., 1999; Okuno et al., 2011; Im et al., 2012). Nari caldera is located at the centre of the island (2.8 km in diameter) and is the source of the most recent phase of activity (< 19 ka; Kim et al., 2014), erupting rocks that range from alkali basalt to trachyandesite in composition (Kim, 1985; Brenna et al., 2014; Chen et al., 2018).

The most recent activity of Ulleungdo is exposed at several outcrops near or within Nari caldera. Machida et al. (1984) defined seven pyroclastic units at extra-caldera outcrops in the north (named in ascending order: U-7 to U-1), which are comprised of trachytic or phonolitic ash and pumice that were emplaced as fall deposits and/or by pyroclastic flows (Figure 2). The Holocene stratigraphy (U-4 to U-2) was further subdivided by Okuno et al. (2011) and Shiihara et al. (2011) at exposures in the southeast, where the units have also been geochemically analysed and radiocarbon dated (Figure 2). Two widespread Japanese tephra marker layers erupted from volcanoes of southern Kyushu Island are found within the soils that formed between these pumice falls, and are named the Aira-Tanzawa (AT; ca. 30.0 ka) and Kikai-Akahoya (K-Ah; ca. 7.3 ka) ash. The U-7 to U-5 eruption units are stratigraphically identified below the AT tephra, and the K-Ah ash is positioned between the U-3 and U-2 eruptions (Shiihara et al., 2011). Radiocarbon dates obtained from buried soils (ca. 2 cm thick) between units, and charred tree material preserved in the Holocene deposits suggest that the U-3 eruption occurred ca. 8.3 or 9 ka BP, respectively, and the U-2 eruption at ca. 5.6 ka BP.

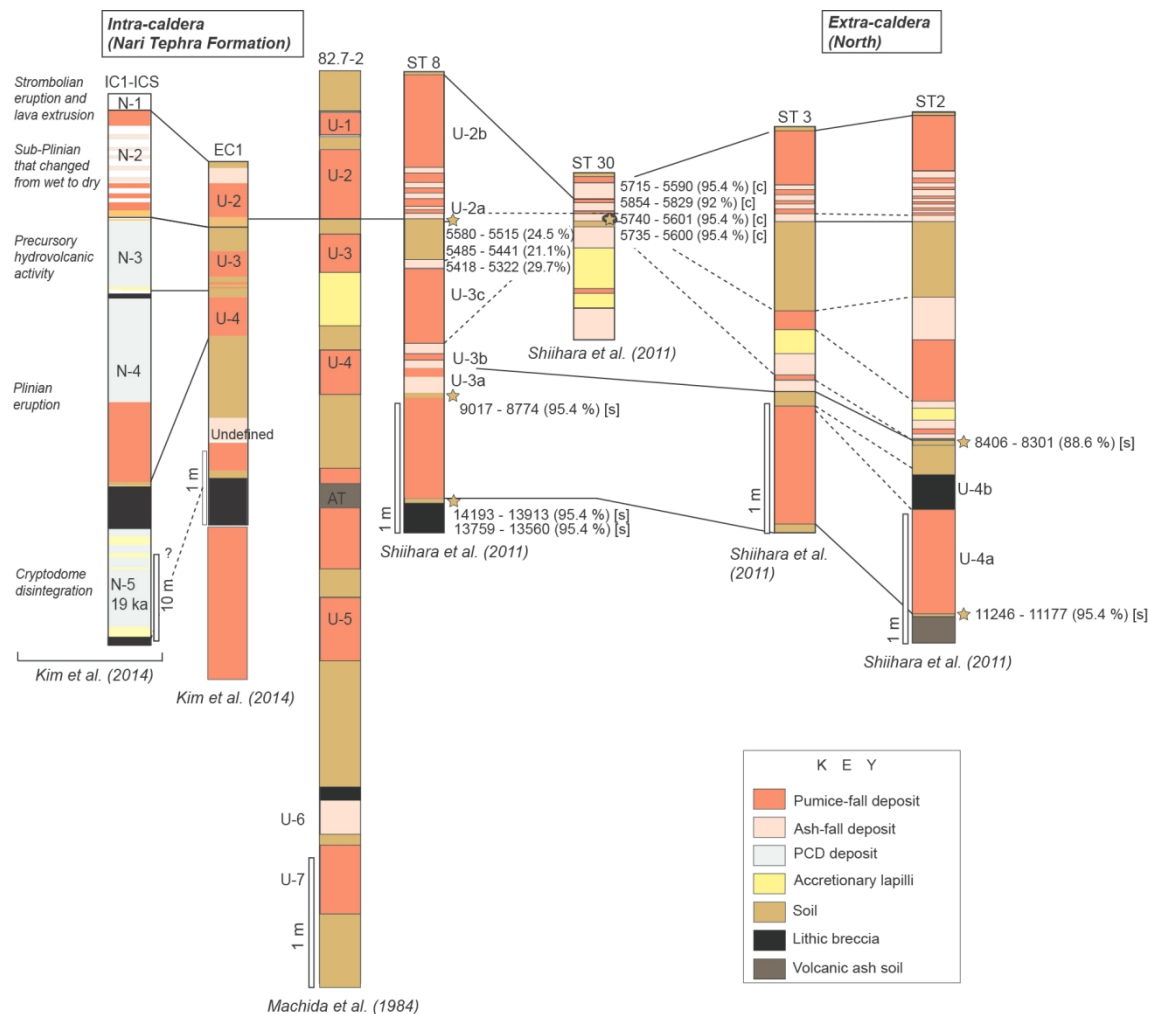


Figure 2. Sedimentological and stratigraphic characteristics of the intra- and extra-caldera outcrops on Ulleungdo Island (Machida et al., 1984; Okuno et al., 2010; Shiihara et al., 2011; Kim et al., 2014). The radiocarbon ages (s = soil; c = charcoal) reported by Okuno et al. (2010) have been recalibrated using IntCal13 (IntCal13 yrs BP). Two Japanese tephra layers erupted from volcanoes in Kyushu are identified within the soils of the extra-caldera sequences, which include the AT (30 ka) and K-Ah (7.3 ka) ash.

Major element glass compositions for Holocene eruptions U-4 to U-2 are known to be geochemically similar (Machida et al., 1984; Martin Jones, 2012; Shiihara et al., 2011). Slight geochemical differences between some subunits are reported by Shiihara et al. (2011), who show that U-4a and U-3c contain glass with lower Al_2O_3 and higher CaO and FeO^T . Furthermore, subunits U-3a and U-

2a are characterised by slightly lower CaO, TiO₂ and FeO^T contents compared to the other units.

Intra-caldera outcrops at Nari are ca. 70 m thick, and are composed of unwelded pyroclastic and epiclastic deposits spanning the last 19 kyrs (Figure 2; Im et al., 2012; Kim et al., 2014). This sequence is named the Nari Tephra Formation, and consists of five key eruptive units (in ascending order, N-5 to N-1), some of which exhibit signs of weathering and soil formation (Figure 2). Several radiocarbon ages have been obtained from this formation by Im et al. (2012), which have been used to correlate the intra- and extra-caldera Holocene deposits (U-4 to U-2, and N-4 to N-2) as shown in Figure 2. Kim et al. (2014) have proposed a detailed succession of eruption styles for the last 19 ka, and suggest that only a few of the events generated sustained eruption columns or pyroclastic density current (PDC) deposits large enough to overtop the caldera wall, and therefore extra-caldera sequences may underestimate the eruption frequency.

2.2. Changbaishan, North Korea/China border

Changbaishan (also referred to as Baitoushan, Paektusan, or Hakutozan) is an intraplate stratovolcano situated on the border of North Korea and China (41°00'N, 128°03'E; Figure 1), located on a Neogene trachybasalt lava shield (the Gaema Plateau). Activity at Changbaishan began in the Middle Pleistocene, and has been divided into three main episodes: early shield building, middle cone construction, and a late explosive stage (Wei et al., 2007; 2013). The most recent of which (< 20 ka) culminated with the caldera-forming

221 Millennium Eruption (ME; VEI 7) which ejected ca. 100 km³ of tephra (Dense
 222 Rock Equivalent ca. 25 km³), blanketing the northernmost regions of Japan in
 223 ash (Horn and Schmincke, 2000; Zou et al., 2010; Wei et al., 2013; Sun et al.,
 224 2014b; McLean et al., 2016) and injecting 45 Tg of sulphur into the atmosphere
 225 (Iacovino et al., 2016). This eruption produced a ca. 4.5 km wide caldera, which
 226 today contains Lake Tianchi (meaning “Heavenly Lake”; Machida et al., 1990).
 227 The age of the ME has been precisely dated to AD 946, by combining
 228 dendrochronology with the presence of a closely related (AD 994) ‘Miyake
 229 event’ (pronounced radiocarbon peak) preserved in charred tree deposits
 230 (Hakozaki et al., 2017; Oppenheimer et al., 2017). The hazard potential of
 231 Changbaishan is considerable and is particularly concerning given that there
 232 has been recent seismic unrest at the crater (Stone, 2010; Xu et al., 2012; Wei
 233 et al., 2013).
 234
 235 The most comprehensively studied proximal outcrop at Changbaishan is at
 236 Twianwenfeng peak, which is on the northern Chinese flank of the summit (e.g.,
 237 Chen et al., 2016; Pan et al., 2017; Sun et al., 2017; 2018). There are many
 238 inconsistent interpretations of these Late Quaternary eruption deposits, even
 239 amongst those assigned to the ME (see Pan et al., 2017). Sun et al. (2017)
 240 identify and geochemically characterise five sequential deposits (oldest to
 241 youngest, named NS-1 to NS-5) at Twianwenfeng peak, and suggest that the
 242 three uppermost units (NS-3 to NS-5) are associated with the ME, due to the
 243 geochemical (major element glass chemistry) overlap with distal ash deposits,
 244 and that no depositional break is evident between units NS-4 and NS-5. This is
 245 in contrast to other studies that suggest that the youngest unit (NS-5) may

246 correlate to post-ME events, which are suggested by historical records in AD
 247 1668 or AD 1702 (Cui et al., 1995; Liu et al., 1998).
 248
 249 The ME had two explosive phases, with the initial main phase (ca. 95% by
 250 volume) associated with a ca. 25 km-high Plinian column, producing a
 251 widespread rhyolitic pumice fall unit (Machida et al., 1990; Horn and
 252 Schmincke, 2000), which equates to NS-3 of Sun et al. (2017). This fall unit is
 253 overlain by partially-welded PDC deposits attributed to the partial collapse of the
 254 Plinian column. Trachytic magma was erupted in a late phase of the eruption
 255 (i.e., NS-4 and NS-5), forming moderately welded PDC units that overlie the
 256 rhyolitic fall and PDC deposits (Horn and Schmincke, 2000). Chen et al. (2016)
 257 report trace element compositions for the ME at Twianwenfeng peak (therein
 258 named units C-3 to C-1), and show that the rhyolitic fall deposits (C-3 to C-2)
 259 had higher contents of incompatible trace elements (e.g., Th, Ta, Nd, Y) and
 260 lower contents of compatible elements (e.g., Ba, Sr) relative to the upper
 261 trachyte unit (C-1).
 262
 263 Sun et al. (2017) identify two pre-ME pyroclastic fall deposits at Twianwenfeng
 264 peak, NS-1 (grey fall unit) and NS-2 (yellow fall unit), which are compositionally
 265 distinct from the ME deposits. These units are estimated to have been erupted
 266 between 4 – 5 ka based on $^{40}\text{Ar}/^{39}\text{Ar}$, uranium series disequilibrium, ^{14}C and
 267 optically stimulated luminescence (OSL) methods (Liu et al., 1998; Wan and
 268 Zheng, 2000; Wang et al., 2001; Yang et al., 2014).
 269

270 A large “lava flow” landform, named the Qixiangzhan Comendite that is 5 km
 271 long and 400-800 m wide, is observed on the northern summit of Changbaishan
 272 (Yang et al., 2014; Sun et al., 2017). This is widely considered as another pre-
 273 ME event, although $^{40}\text{Ar}/^{39}\text{Ar}$ ages generated from this deposit span several
 274 thousand years (e.g., Singer et al., 2014; Yang et al., 2014) and its stratigraphic
 275 relationship to the units preserved at Twianwenfeng peak is unclear (Sun et al.,
 276 2017). Major element glass compositions of the Qixiangzhan comendite overlap
 277 with those of the rhyolitic phase of the ME (Sun et al., 2018).

278

279 *2.3. Distal marine and lacustrine tephra records*

280

281 The Sea of Japan (East Sea) is a semi-enclosed marginal sea located between
 282 the Japanese islands and the Asian continent, and is the product of the rear-arc
 283 extension (Figure 1). Due to the prevailing westerly winds, tephra erupted from
 284 Ulleungdo and Changbaishan is typically dispersed to the east and deposited in
 285 the surrounding marine basins (Arai et al., 1981; Chun et al., 1997, 2007;
 286 Ikehara, 2003; Machida and Arai, 2003; Ikehara et al., 2004; Lim et al., 2013,
 287 2014; Derkachev et al., in press). Furthermore, several Japanese tephra layers
 288 erupted from volcanoes on Kyushu Island have been dispersed to, and
 289 deposited in the Sea of Japan, including the K-Ah (Kikai), AT (Aira), SAN1
 290 (Kuju) and Aso-4 eruption deposits (Machida and Arai, 2003; Albert et al.,
 291 2019). The marine sediments across the Sea of Japan are characterised by
 292 alternations of light and dark coloured sediments, which have been attributed to
 293 millennial-scale palaeoenvironmental changes associated with changes in the
 294 East Asian summer monsoon (Tada, 1999; Ikehara, 2003). These organic rich

dark-layers are commonly used to date tephra layers that are preserved in the marine sediments (Tada et al., 1999). It has proved very difficult to correlate between the proximal eruption successions exposed at Ulleungdo and Changbaishan with those in distal records (Shiuhara et al., 2011; Kim et al., 2014; Chen et al., 2016; Pan et al., 2017). Typically, only the largest Holocene eruptions that reached the Japanese islands have been correlated to specific eruption units within proximal stratigraphies of these two volcanoes.

The most widespread tephra layer from Changbaishan is associated with the AD 946 ME, and is distally named the Baegdusan-Tomakomai (B-Tm tephra). The B-Tm tephra was named and characterised using glass refractive indices and major element compositions (Machida and Arai, 1983; McLean et al., 2016) at a distal type-locality in Tomakomai Port, Hokkaido (northern Japan), where it was identified above the Tarumai-c (ca. 50 BC) and below the Tarumai-b (AD 1667) tephra layers from the nearby Tarumae volcano (Machida and Arai, 1983). The B-Tm tephra has since been identified in numerous marine, lacustrine and archaeological sequences across northern Japan, northeast China and coastal regions of Russia (see Sun et al., 2014b; McLean et al., 2016) and B-Tm glass shards have been identified in the Greenland ice cores (Sun et al., 2014a).

The most widespread tephra erupted from Ulleungdo is the Ulleung-Oki (U-Oki), which is correlated to the proximal U-4 deposits on the island (Machida et al., 1984; Okuno et al., 2010; Shiuhara et al., 2011; Smith et al., 2011; Kim et al., 2014). The U-Oki tephra has been identified in several marine cores in the Sea

of Japan, and in archives on the islands of Japan, including Lake Biwa, Lake Suigetsu and Lake Hane (Chun et al., 1997; Domitsu et al., 2002; Nagahashi et al., 2004; Smith et al., 2011; Figure 1). As outlined further below, several of these archives contain a younger phonolitic/trachytic ash that post-dates the U-Oki tephra, and are thought to be distal correlatives of the U-3 eruption of Ulleungdo.

One of the most comprehensive records of East Asian volcanism is the Lake Suigetsu sedimentary archive, which is located ca. 500 km E of Ulleungdo and ca. 1000 km SSE of Changbaishan (35°35'0"N, 135°53'0"E, 0 m above present sea level; Figure 1). The sequence spans approximately 150 ka (Nakagawa et al., 2012), and contains a detailed record of visible and non-visible (cryptotephra) layers derived from Ulleungdo and Changbaishan eruptions, as well as over thirty visible tephra layers erupted from sources that span the length of Japan (Smith et al., 2013; McLean et al., 2016, 2018; Albert et al., 2018, 2019). Despite the difficulties of identifying non-visible layers in a productive arc setting, cryptotephra layers are precisely preserved and identified in Lake Suigetsu, partially due to its unique hydrological setting. Suigetsu is a tectonic lake, adequately situated away from the large calderas in Hokkaido and Kyushu, and so is not inundated with locally sourced volcanic glass which would preclude the identification of cryptotephra layers deposited during large distally occurring eruptions. Furthermore, no rivers flow directly into Lake Suigetsu (Figure 1b) with the water level controlled by input into the other connected lakes. The fine-grain sedimentation in the lake is often interrupted by deposits of coarse volcanic ash that fall through the water column.

Since the Lake Suigetsu sediments have been extensively radiocarbon (^{14}C) dated, and seasonal laminae (varves) are preserved between ca. 10 and 50 ka (Staff et al., 2011; Bronk Ramsey et al., 2012; Marshall et al., 2012; Schlolaut et al., 2012), eruptions within the radiocarbon timeframe can be precisely dated if their associated tephra layers are identified. The Lake Suigetsu tephrostratigraphic record is therefore utilised in this study to precisely date ash fall events of Ulleungdo and Changbaishan that reached central Honshu, and integrate their tephrostratigraphies.

3. Tephra identification and analytical methods

3.1. New tephra identification in Lake Suigetsu

The high-resolution and intensely dated sediments of Lake Suigetsu (SG06 and SG14 cores) have been re-investigated for the presence of thin (i.e., sub millimetre in thickness) and cryptotephra layers, in order to supplement the visible tephrostratigraphy as introduced above, and published by Smith et al., (2011, 2013) and Albert et al. (2018, 2019). Cryptotephra extraction procedures (modified from Turney, 1998; Blockley et al., 2005) were undertaken through the 12 m of Holocene sediments (≤ 10 ka; McLean et al., 2016, 2018) and more recently the 14 m of annually laminated (varved) sediments dating to between ca. 50 and 30 ka. These sections were chosen for analysis as they were expected to contain low-background levels of volcanic glass, which would not obscure primary cryptotephra peaks (see McLean et al., 2018). On average,

through these investigated sediments cryptotephra layers are four times more frequently preserved than visible ash layers. Identified tephra layers in the Suigetsu sediments are named, and are referred to using their SG06 (correlation model 06 June '17) or SG14 (correlation model 30 May '16) core composite depth(s) in cm.

The Suigetsu Bayesian age model (Staff et al., 2011; Bronk Ramsey et al., 2012) was used to determine the age for ash layers preserved in the sediments. The composite Suigetsu sedimentary sequence was modelled on to the IntCal13 timescale (Reimer et al., 2013) implementing three successive cross-referenced Poisson-process ('P_Sequence') depositional models using OxCal (ver. 4.3; Bronk Ramsey, 2008, 2017). These include 775 AMS ¹⁴C dates obtained from terrestrial plant macrofossils from the upper 38 m (SG06-Composite Depth (CD) of the SG93 and SG06 cores (Kitagawa and van der Plicht, 1998a; 1998b, 2000; Staff et al., 2011, 2013a, 2013b; Bronk Ramsey et al., 2012) and varve counting between 12.88 and 31.67m SG06 CD (Marshall et al., 2012; Schlolaut et al., 2012). Outside of the varve-counted depth interval, SG06 event-free depth(s) (EFD, ver. 29th Jan '11) were used within the age model, which excludes instantaneous deposits > 5 mm in thickness, (e.g., floods, and tephra deposits; Staff et al., 2011; Schlolaut et al., 2012).

3.2. Major and trace element analysis of the glass shards

Major and minor element compositions of individual glass shards extracted from the Suigetsu visible and cryptotephra layers were measured using a JEOL-8600

961
962
963 395 wavelength-dispersive electron microprobe (WDS-EMP) at the Research
964
965 396 Laboratory for Archaeology and History of Art (RLAHA), University of Oxford. All
966
967 397 glass analyses used an accelerating voltage of 15 kV, beam current of 6 nA and
968
969 398 10 μm -diameter beam. Peak counting times were 12 s for Na, 50 s for Cl, 60 s
970
971 399 for P, and for 30 s for all other elements. The electron microprobe was
972
973 400 calibrated using a suite of mineral standards, and the PAP absorption correction
974
975 401 method was applied for quantification. The accuracy and precision of these data
976
977 402 were assessed using analyses of the MPI-DING reference glasses from the
978
979 403 Max Plank Institute (Jochum et al., 2006), which were run as secondary
980
981 404 standards. Analyses of these secondary standards lie within the standard
982
983 405 deviation of the preferred values and are presented in the Supplementary
984
985 406 Material. All these data were filtered to remove non-glass analyses, and those
986
987 407 with low analytical totals <93%. The raw values were normalised (to 100 %) for
988
989 408 comparative purposes and to account for variable glass hydration, and are
990
991 409 presented as such in all tables and figures.
992
993
994
995
996

997 411 Trace element compositions of the glass shards >25 μm (i.e. large enough for
998
999 412 analysis) were measured by laser ablation inductively-coupled plasma mass
1000
1001 413 spectrometry (LA-ICP-MS) at the Department of Solid Earth Geochemistry,
1002
1003 414 Japan Agency for Marine-Earth Science and Technology (JAMSTEC). The
1004
1005 415 analytical equipment used include the deep-ultraviolet (200 nm) femtosecond
1006
1007 416 laser ablation system (DUV-FsLA) of OK-Fs2000K (OK Laboratory, Tokyo,
1008
1009 417 Japan) connected to the modified high-sensitivity sector field ICP-MS of
1010
1011 418 Element XR (Thermo Scientific, Bremen, Germany). All analyses used a 25 μm
1012
1013 419 crater diameter and depth, and conditions followed those reported by Kimura
1014
1015
1016
1017
1018
1019
1020

and Chang (2012). Ten major elements including P_2O_5 and 33 trace elements were analysed for each sample, and were also run alongside several MPI-DING reference glasses (Jochum et al., 2006), and the BHVO-2G standard provided by the United States Geological Survey. Accuracies of the BHVO-2G glass analyses are typically < 3 % for most elements, < 5 % for Sc, Ga, Sm, Eu, Gd, U and < 10 % for Ni, Cu, Lu. Full trace element datasets and secondary standard analyses are provided in the Supplementary Material.

4. Results

4.1. Suigetsu tephrostratigraphy

To date, thirty-three visible tephra layers (Smith et al., 2011, 2013; Albert et al., 2018; 2019; McLean et al., 2016, 2018) and thirty-four cryptotephra layers (between 50 to 30 ka, and > 10 ka; McLean et al., 2018) have been identified and geochemically fingerprinted in the Lake Suigetsu sediments. The distinctively high alkali content of glass shards ($Na_2O + K_2O = > 9$ wt. %; Figure 3) of eight of these tephra layers indicates that they are not from the Japanese arc volcanoes (Machida and Arai, 2003; Kimura et al., 2015; Albert et al., 2019), and are correlated by McLean et al. (2016, 2018; $n = 6$) and herein ($n = 2$) to eruptions from Ulleungdo and Changbaishan.

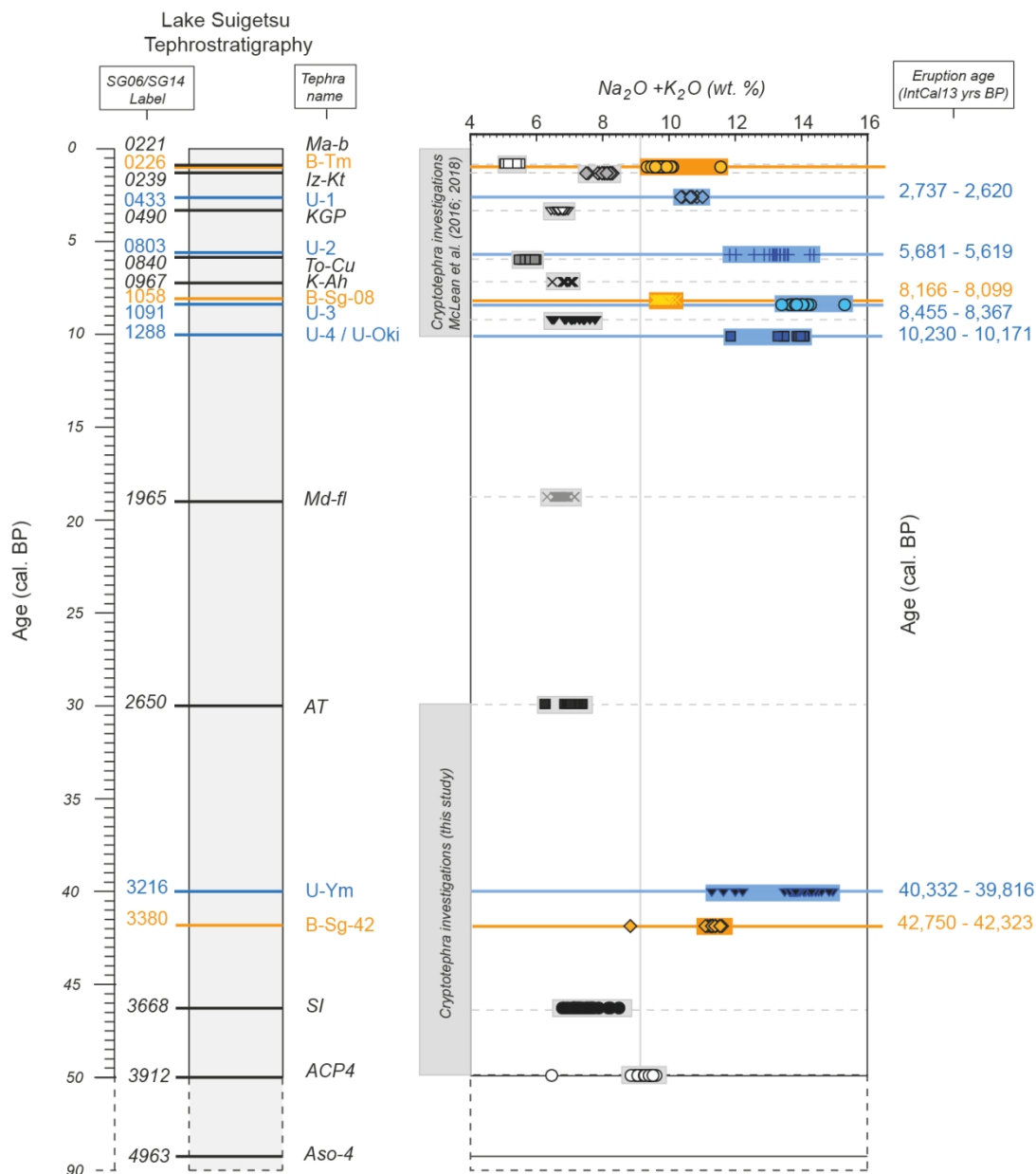


Figure 3. The composite Lake Suigetsu tephrostratigraphy and the positioning of Ulleungdo (blue lines), Changbaishan (orange) and other key Japanese (black/grey) tephra layers preserved through the sequence (Smith et al., 2013; McLean et al., 2016, 2018; Albert et al., 2018; 2019). The glass shard total alkali content (Na₂O + K₂O) of these layers is also plotted against eruption age, with Ulleungdo and Changbaishan tephras containing > 9 wt. %.

4.1.1. New Ulleungdo and Changbaishan deposits

As part of detailed cryptotephra investigations through the Suigetsu sediments dated between ca. 50 to 30 ka, two new alkaline ash layers named SG14-3380 and SG14-3216 have been identified. These are positioned between the Sambe-Ikeda (46.4 ka; Albert et al., 2019) and AT (30.0 ka; Smith et al, 2013; Albert et al., 2019) tephras (Figure 3; Table 1). SG14-3380 is a highly concentrated cryptotephra horizon erupted from Changbaishan, and contains over 18,000 shards per gram of dried sediment (Figure 4a.). This eruption is dated to between 42,750 – 42,323 IntCal13 yrs BP (95.4 % confidence interval) using the Suigetsu age model. SG14-3216 is a thin visible (ca. 1 mm) white ash layer (Figure 4b) that is ca. 1.6 m above SG14-3380, and represents an Ulleungdo eruption between 40,332 – 39,816 IntCal13yrs BP (95.4 % confidence interval).

4.1.2. Previous identifications of Ulleungdo and Changbaishan deposits

As previously reported by McLean et al. (2018), the Lake Suigetsu Holocene tephrostratigraphy contains three eruptions from Ulleungdo: SG06-1288, SG14-1091 and SG14-0803 that are dated to 10,230 – 10,171 IntCal13 yrs BP, 8,455 – 8,367 IntCal13 yrs BP and 5,681 – 5,619 IntCal13 yrs BP (95.4 % confidence interval), respectively (Table 1; Figure 3; Smith et al., 2011; McLean et al., 2018). A younger ash layer that also has glass compositions that are similar to eruptions from Ulleungdo (SG14-0433) is dated to 2,737 – 2,620 IntCal13 yrs BP (Table 1; Figure 3).

Table 1. Summary of the Ulleungdo and Changbaishan derived tephra layers identified in the Lake Suigetsu (SG06 & SG14) sequence (in bold and shaded grey), along with their stratigraphic positioning relative to key Japanese marker layers. Tephra correlations for SG06 tephra layers are discussed by Smith et al. (2013), McLean et al. (2016) and Albert et al. (2018, 2019) and SG14 tephra layers are correlated in McLean et al. (2018, this study).

SG Label	Tephra code	Tephra name	Source volcano	Source location	¹⁴ C date (AD / IntCal13 yrs BP)
SG14-0221	Ma-b	Mashu-b	Mashu	Kurile arc, Japan	AD 960 - 992 ¹
SG06-0226	B-Tm	Baegdusan-Tomakomai	Changbaishan	North Korea / China	AD 946²
SG14-0239	Iz-Kt	Izu-Kozushima-Tenjosan	Kozushima	Izu arc, Japan	AD 838 ³
SG14-0433	U-1	Ulleung-1	Ulleungdo	South Korea	2,737 - 2,620¹
SG14-0490	KGP	Kawagodaira Pumice	Kawagodaira	Izu arc, Japan	3,227 - 3,129 ¹
SG14-0803	U-2	Ulleung-2	Ulleungdo	South Korea	5,681 - 5,619¹
SG14-0840	To-Cu	Towada-Chuseri	Towada	Northern Honshu, Japan	5,986 - 5,899 ¹
SG06-0967	K-Ah	Kikai-Akohoya	Kikai	Southern Kyushu, Japan	7,307 - 7,196 ¹
SG14-1058	B-Sg-08	Baegdusan-Suigetsu-08	Changbaishan	North Korea / China	8,166 - 8,099¹
SG14-1091	U-3	Ulleung-3	Ulleungdo	South Korea	8,455 - 8,367¹
SG14-1185	1185	-	-	-	9,372 - 9,301 ¹
SG06-1288	U-Ok / U-4	Ulleung-4 / Ulleung-Ok	Ulleungdo	South Korea	10,230 - 10,171¹
SG06-1965	Md-fl	Sambe-Midorigaoka fl	Sambe	SW Japan	19,631 - 19,471 ⁴
SG06-2650	AT	Aira-Tanzawa	Aira	Southern Kyushu, Japan	30,174 - 30,078 ⁴
SG14-3216	U-Ym	Ulleung-Yamato	Ulleungdo	South Korea	40,332 - 39,816⁵
SG14-3380	B-Sg-42	Baegdusan-Suigetsu-42	Changbaishan	North Korea / China	42,750 - 42,323⁵
SG06-3668	SI	Sambe-Ikeda	Sambe	SW Japan	46,566 - 46,162 ⁴
SG06-3912	ACP4	Aso-Central Pumice 4	Aso	Central Kyushu, Japan	50,311 - 49,637 ⁴
SG06-4963	Aso-4	Aso-4	Aso	Central Kyushu, Japan	86.4 ± 1.1 ⁴⁰ Ar/ ³⁹ Ar ⁴

1) McLean et al. (2018); 2) Oppenheimier et al. (2017); Hakozaiki et al., 2017; 3) Tsukui et al. (2006); 4) Smith et al. (2013); Albert et al. (2019); 5) This study

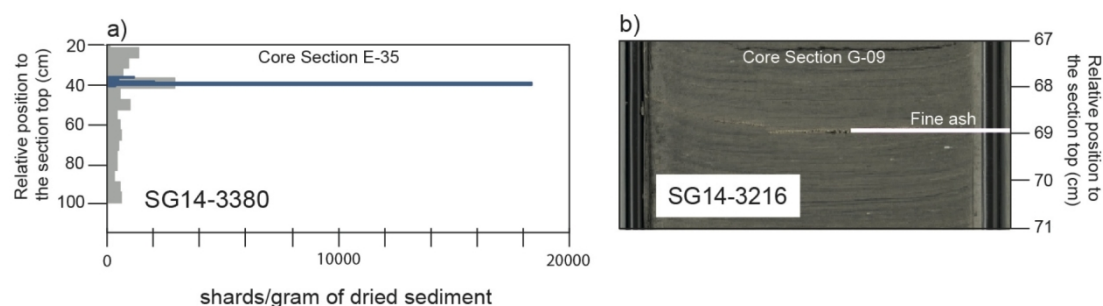


Figure 4. (a) Glass shard concentrations (shards per gram of dry sediment) preserved in SG14 core E-35 and the positioning of cryptotephra SG14-3380. Concentration of low-resolution (5 cm) samples are shown in grey and high-resolution samples (1 cm) are overlain in blue. Shard counts for the other Holocene cryptotephra layers are published by McLean et al. (2018). (b) Photograph of visible tephra layer SG14-3216 in Lake Suigetsu Core G-09.

Two Holocene Changbaishan eruptions are preserved in the sediments: SG14-1058 at 8,166 – 8,099 IntCal13 yrs BP (McLean et al., 2018); and SG06-0226, which has been correlated to the AD 946 B-Tm tephra from the ME (McLean et al., 2016; Hakozaiki et al., 2017; Oppenheimer et al., 2017). Several other widespread markers have been identified in the Holocene sediments, which are able to stratigraphically separate eruption events from Ulleungdo and Changbaishan (Figure 3; Table 1). SG14-1185 stratigraphically separates the SG06-1288 and SG14-1091 Ulleungdo layers, and the K-Ah (7.3 ka; Kikai volcano) and To-Cu (5.9 ka; Towada) tephra layers separate SG14-1091 and SG14-0830 (McLean et al., 2018; Table 1; Figure 3).

4.2. Major and trace element volcanic glass geochemistry

4.2.1. Ulleungdo glass geochemistry

The newly analysed glass of SG14-3216 geochemically overlaps with the other previously identified Ulleungdo derived tephra layers preserved in the Suigetsu tephrostratigraphy (e.g., SG06-1288, SG14-1091 and SG14-0803). Collectively they straddle the phonolitic/trachytic boundary on the basis of the Total Alkalis versus Silica (TAS) classification (Le Bas et al., 1986) and contain 60 – 63 wt. % SiO₂, ca. 7 wt. % K₂O and 19 – 20 wt. % Al₂O₃ (Table 2; Figure 5). These glasses are characterised by < 2.5 wt. % CaO and contain between 2.5 and 3.5 wt. % FeO^T.

513 When normalised to the primitive mantle (Sun and McDonough, 1989), we find
 514 the newly obtained trace element compositions of SG14-3216 and SG14-1091
 515 show enrichments in the Light Rare Earth Elements (LREE) relative to the
 516 Heavy Rare Earth Elements (HREE) ($\text{La/Yb} = 30 - 35$ ppm) and significant
 517 depletions in Ba, Sr and Eu that reflect K-feldspar fractionation (Figure 6). The
 518 paucity of a depletion in Nb and Ta content within these volcanic glasses, when
 519 normalised to the primitive mantle, is inconsistent with subduction related
 520 volcanism (Figure 6).
 521
 522 The four tephra layers with Ulleungdo compositions are difficult to distinguish
 523 using their major element glass compositions, but we find that the younger
 524 glasses of SG14-0803 are more elevated in CaO (by ca. 0.5 wt. %), compared
 525 to the early Holocene and SG14-3216 glass (Figure 5c). In addition, the alkaline
 526 glasses of SG14-3216 (59.5 – 62.5 wt. % SiO_2 and total alkalis [$\text{Na}_2\text{O} + \text{K}_2\text{O}$] of
 527 11.6 – 14.9 wt. %) can be discriminated from SG14-1091 by larger feldspar-
 528 related depletions in Sr, Ba and Eu, that are normalised to primitive mantle
 529 compositions (Figure 6). The alkaline glass shards of SG14-0433 ($\text{Na}_2\text{O} + \text{K}_2\text{O}$
 530 = 10.4 – 11.0) are also likely to derive from Ulleungdo, but contain ca. 2.5 wt. %
 531 lower K_2O , and ca. 2 wt. % higher CaO compared to the older eruption events
 532 outlined here (Figure 5a; 5c).

Table 2. Average major, minor and trace element glass compositions of the Ulleungdo and Changbaishan tephra layers in the Lake Suigetsu sediment core.

wt. (%)	SG14-0433		SG14-0803		SG14-1091		SG06-1288		SG14-3216	
	McLean et al. 2018		McLean et al. 2018		McLean et al. 2018		Smith et al. 2011		this study	
	Mean	±1σ	Mean	±1σ	Mean	±1σ	Mean	±1σ	Mean	±1σ
SiO ₂	61.76	0.16	60.54	0.63	60.52	0.24	60.85	0.42	60.75	0.67
TiO ₂	0.79	0.05	0.62	0.07	0.51	0.08	0.50	0.07	0.39	0.07
Al ₂ O ₃	16.66	0.05	19.48	0.30	19.87	0.22	19.55	0.17	19.85	0.28
FeO ^T	5.65	0.17	3.16	0.42	2.77	0.24	3.16	0.19	3.12	0.16
MnO	0.23	0.05	0.14	0.10	0.15	0.03	0.14	0.05	0.18	0.05
MgO	1.09	0.06	0.48	0.12	0.23	0.03	0.30	0.06	0.17	0.07
CaO	6.07	0.18	6.60	0.60	6.95	0.40	1.61	0.17	1.34	0.12
Na ₂ O	2.57	0.08	1.99	0.33	1.48	0.14	6.51	0.79	7.28	0.96
K ₂ O	4.59	0.10	6.61	0.21	7.03	0.19	7.07	0.28	6.50	0.33
P ₂ O ₅	0.36	0.04	0.17	0.05	0.05	0.04	0.10	0.03	0.05	0.03
Cl	0.23	0.03	0.21	0.04	0.40	0.08	0.24	0.03	0.37	0.10
Analytical total	96.85		96.84		97.81		99.72		97.03	
n	8		19		24		12		37	
wt. (%)	SG06-0226		SG14-1058		SG14-3380					
	McLean et al. 2016		McLean et al. 2018		this study					
	Mean	±1σ	Mean	±1σ	Mean	±1σ				
SiO ₂	74.89	0.21	75.01	0.18	66.26	0.70				
TiO ₂	0.22	0.04	0.20	0.03	0.60	0.09				
Al ₂ O ₃	10.27	0.10	10.28	0.11	14.97	0.28				
FeO ^T	4.05	0.14	3.89	0.10	5.12	0.14				
MnO	0.08	0.05	0.07	0.03	0.15	0.04				
MgO	0.02	0.03	0.01	0.01	0.25	0.06				
CaO	0.22	0.02	5.30	0.16	1.24	0.17				
Na ₂ O	5.36	0.15	0.20	0.02	5.67	0.66				
K ₂ O	4.38	0.09	4.50	0.06	5.49	0.09				
P ₂ O ₅	-	-	0.01	0.01	0.09	0.03				
Cl	0.50	0.03	0.52	0.02	0.16	0.02				
Analytical total	96.19		95.54		95.90					
n	29		24		14					

ppm	SG06-0226		SG14-1058		SG14-1091		SG14-3216		SG14-3380	
	this study		this study		this study		this study		this study	
	Mean	±1σ	Mean	±1σ	Mean	±1σ	Mean	±1σ	Mean	±1σ
Rb	396.4	9.8	383.9	23.9	188.7	10.1	195.4	19.1	143.5	8.9
Sr	2.2	0.6	4.4	0.9	59.5	36.2	14.3	10.2	25.0	24.4
Y	143.3	3.9	149.8	11.4	23.5	2.0	26.0	2.9	51.1	3.9
Zr	2415.2	80.0	2302.5	189.8	626.0	50.9	709.6	104.3	741.4	45.8
Nb	286.1	8.9	261.1	21.1	169.8	11.5	175.2	21.2	97.0	5.5
Ba	6.4	0.9	6.6	2.5	99.1	83.5	16.3	13.3	77.3	57.3
La	138.9	4.5	125.2	14.6	86.4	4.3	98.2	9.0	76.4	4.7
Ce	286.9	13.5	243.2	12.3	144.8	6.9	161.7	15.7	154.3	9.6
Pr	31.9	1.2	28.3	1.8	12.8	0.9	14.5	1.2	17.1	1.1
Nd	115.8	4.8	102.3	6.9	39.3	3.5	43.9	4.7	65.6	6.4
Sm	27.6	1.2	26.1	4.5	5.6	1.0	6.4	0.7	12.9	1.9
Eu	0.3	0.1	0.3	0.3	1.5	0.3	0.6	0.2	0.6	0.2
Gd	26.7	1.5	28.0	3.3	5.0	1.4	5.4	1.9	10.7	1.4
Dy	25.3	1.8	25.5	2.2	3.8	0.6	4.4	0.6	9.3	0.9
Er	14.0	0.6	14.0	1.6	2.5	0.5	2.8	0.6	5.1	0.7
Yb	11.4	0.5	11.2	2.0	2.6	0.4	3.1	0.7	4.3	0.6
Hf	55.6	2.3	55.6	5.4	12.0	1.1	13.4	2.1	16.9	1.2
Ta	17.0	1.1	16.4	1.9	9.8	0.7	9.7	1.1	5.6	0.5
Th	49.9	3.1	49.6	5.0	23.5	1.9	25.2	3.2	14.1	1.1
U	10.8	0.7	9.7	0.9	4.8	0.5	5.3	0.9	2.8	0.3
Y/Th	2.9	0.2	3.0	0.1	1.0	1.1	1.0	0.1	3.6	0.2
Zr/Th	48.5	2.5	46.5	2.0	26.6	27.5	28.1	2.3	52.6	3.3
La/Yb	12.1	0.4	11.3	1.4	34.4	6.5	32.7	4.9	18.0	2.4
n	8		5		13		8		10	

(FeO^T = all Fe reported as FeO). Raw dataset and secondary standards are included in the Supplementary Material.

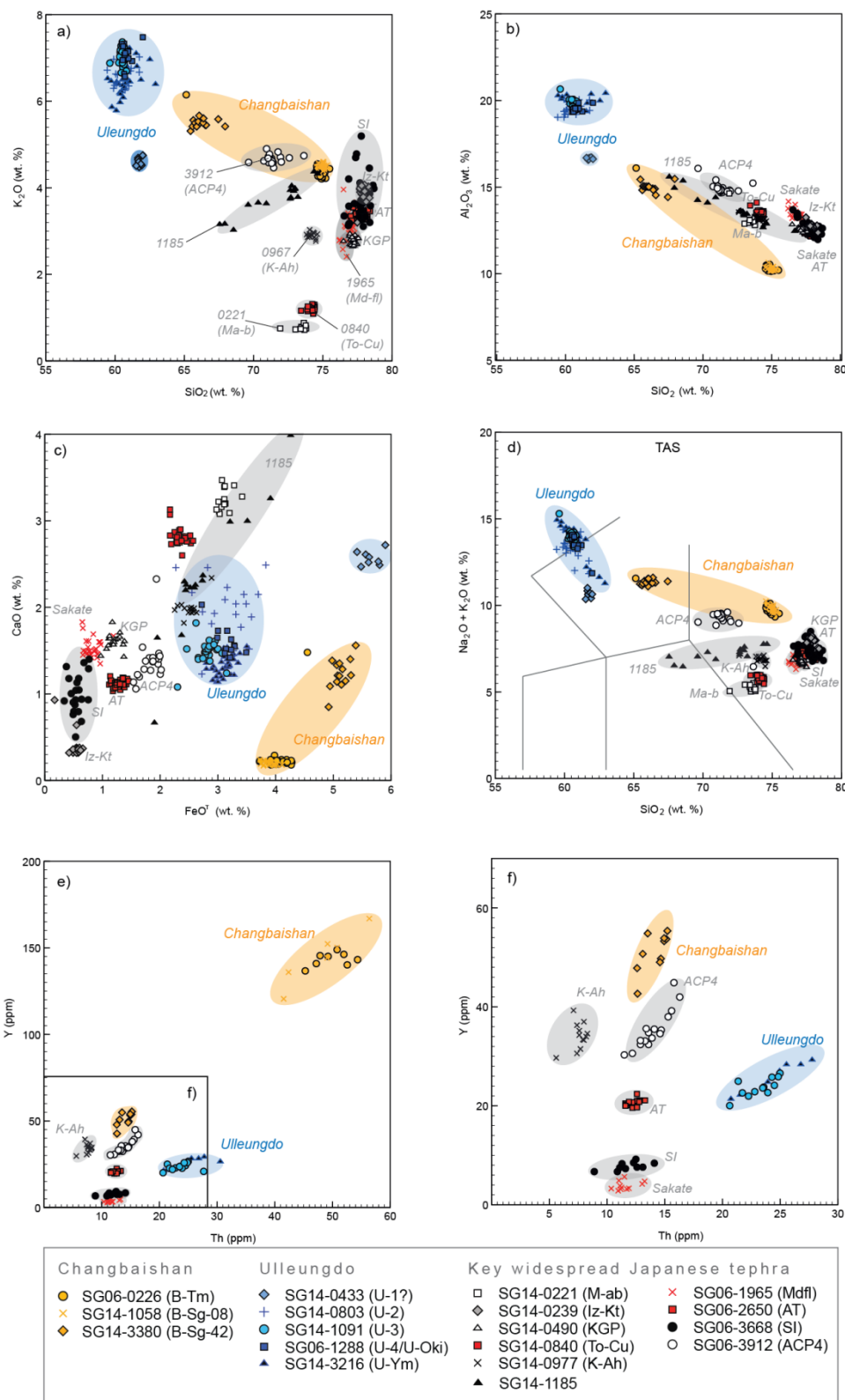


Figure 5. Glass shard major (5a – d) and trace (5e – f) element compositions of Ulleungdo (South Korea; shown in blue), Changbaishan (North Korea/China; shown in orange), and key Japanese tephras layers that are preserved in the Lake Suigetsu sediments (shown in grey and black) (Smith et al., 2013; McLean et al., 2016, 2018; Albert et al., 2018, 2019). (d) Total alkali versus silica plot (TAS) with whole-rock classification based on Le Bas et al., 1986).

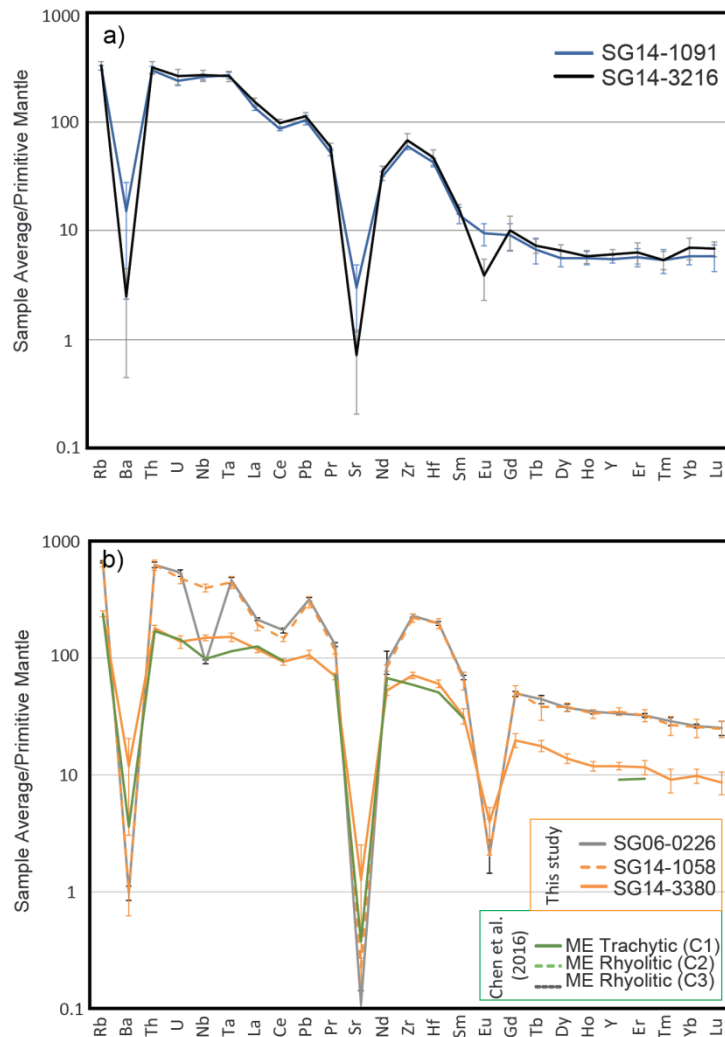


Figure 6. Primitive mantle normalised trace element compositions of glasses of: (a) Ulleungdo tephra layers (SG14-1091 and SG14-3216) in the Lake Suigetsu sequence; (b) Changbaishan tephra layers (SG06-0225, SG14-1058 and SG14-3380) in comparison to proximal ME rhyolitic (C2 – C3) and trachytic (C1) proximal deposits (Chen et al., 2016). Primitive mantle values follow Sun and McDonough (1989).

4.2.2. Changbaishan glass geochemistry

The three Changbaishan derived tephra layers (e.g., SG14-3380, SG14-1058 and SG06-0226) contain both rhyolitic and trachytic glass compositions ($\text{Na}_2\text{O} + \text{K}_2\text{O} = > 9.5$ wt. %; Le Bas et al., 1986), with SiO_2 ranging from 65.5 to 75.5 wt. % (Table 2; Figure 5d). They contain < 1.6 wt. % CaO, and between 3.7 and 5.4 wt. % FeO^{T} (Figure 5c). New trace element analyses indicate that when

normalised to primitive mantle compositions, all glasses are enriched in LREE relative to HREE, with La/Yb ratios higher in those of SG14-3880, relative to SG14-1058 and SG06-0226 (Table 2) and show pronounced negative feldspar-related anomalies in Ba, Sr and Eu (Figure 6).

The newly analysed glasses of SG14-3380 are exclusively trachytic (65.4 – 67.9 wt. % SiO₂, 14.4 – 15.5 wt. % Al₂O₃, and Na₂O + K₂O = 8.7 – 11.7 wt. %) and are compositionally similar to the single trachytic analysis from SG06-0226. Trace element compositions for SG14-3380 are homogenous with 14.1 ± 1.1 ppm Th, 144 ± 9.0 ppm Rb, and 51 ± 4 ppm Y (Table 2). Unfortunately, no trace elements could be obtained for the trachytic end-member of SG06-0226 for further comparison with SG14-3380.

As discussed by McLean et al. (2018), the rhyolitic SG06-0226 glass compositions overlap with SG14-1058 for all major elements (Table 2; Figure 5). Both tephra contain glass compositions that are geochemically homogenous, with ca. 75 wt. % SiO₂, 10.3 wt. % Al₂O₃ and ca. 4.4 wt. % K₂O, and are characterised by very low CaO concentrations (< 0.3 wt. %). The newly generated trace element compositions of SG14-0226 and SG06-1058 show significant overlap, and are more enriched in incompatible elements (e.g., Th, Ta and Y), whilst depleted in compatible elements (e.g., Sr, Ba, and Eu) relative to the trachytic glass of SG14-3380 (Table 2; Figure 6b). SG06-0226 and SG14-1058 have similar mantle normalised profiles and levels of incompatible trace element enrichment (Figure 6). Glasses of both tephra layers have greater feldspar-related depletions in Ba, Sr and Eu relative to SG14-3380. The SG06-0226 glasses show a significant depletion in Nb, which is not observed in

584 SG14-1058 and SG14-3380, which given the intraplate setting of the volcano
585 may relate to late stage, high-level fractionation processes.

586

587

588 **5. Review of Ulleungdo and Changbaishan eruption framework**

589

590 Here, the distal ash deposits erupted from Ulleungdo and Changbaishan are
591 outlined and reviewed using the relative stratigraphy, geochemical glass
592 compositions and eruption chronology. Published occurrences are centred on
593 the Lake Suigetsu tephrostratigraphy to provide an integrated framework that is
594 constrained by numerous widespread ash layers erupted from Japanese
595 volcanoes (Figure 7). There are no pre-50 ka visible ash layers in Lake
596 Suigetsu with Ulleungdo or Changbaishan compositions, but we should
597 highlight that cryptotephra extraction techniques have not yet been carried out
598 on these older sediments. It is possible that there are other pre-50 ka Ulleungdo
599 or Changbaishan layers preserved cryptically in Lake Suigetsu.



Reference(s):

5.1. Ulleungdo eruption history

Ulleungdo has erupted explosively at least five times over the last 86 kyrs (since the eruption of the Aso-4 tephra) with associated widespread ash fall events recognised by the ca. 60 – 61 ka U-Sado tephra (Lim et al., 2013); the ca. 40.1 ka U-Ym tephra (*this study*); the ca. 10 ka U-Oki/U-4 tephra (Smith et al., 2011; 2013); ca. 8.4 ka U-3 tephra (McLean et al., 2018); and the ca. 5.7 ka U-2 tephra (McLean et al., 2018). The known distal deposits of these events and possible proximal correlations are illustrated in Figure 7 and discussed further below.

5.1.1. Post 86 ka (Aso-4) Ulleungdo eruptions

Distal ash layers erupted from Ulleungdo were identified stratigraphically below the AT tephra (30 ka) in marine sediments obtained from the Oki ridge (Arai et al., 1981) and Yamato Basin (Ikehara et al., 2004). These pre-AT Ulleungdo tephra layers were originally considered to be from a single eruption, but the age was controversial. However, Chun et al. (2007) clarified the issue by identifying two separate alkaline ash deposits in marine core MD01-2407 (Figure 1), which they named SKPI and SKPII, and were dated to 40 – 41 ka and 60 – 61 ka, respectively, based on correlations with the regional-scale thinly-laminated marine stratigraphy (Tada, 1999; Chun et al., 2007).

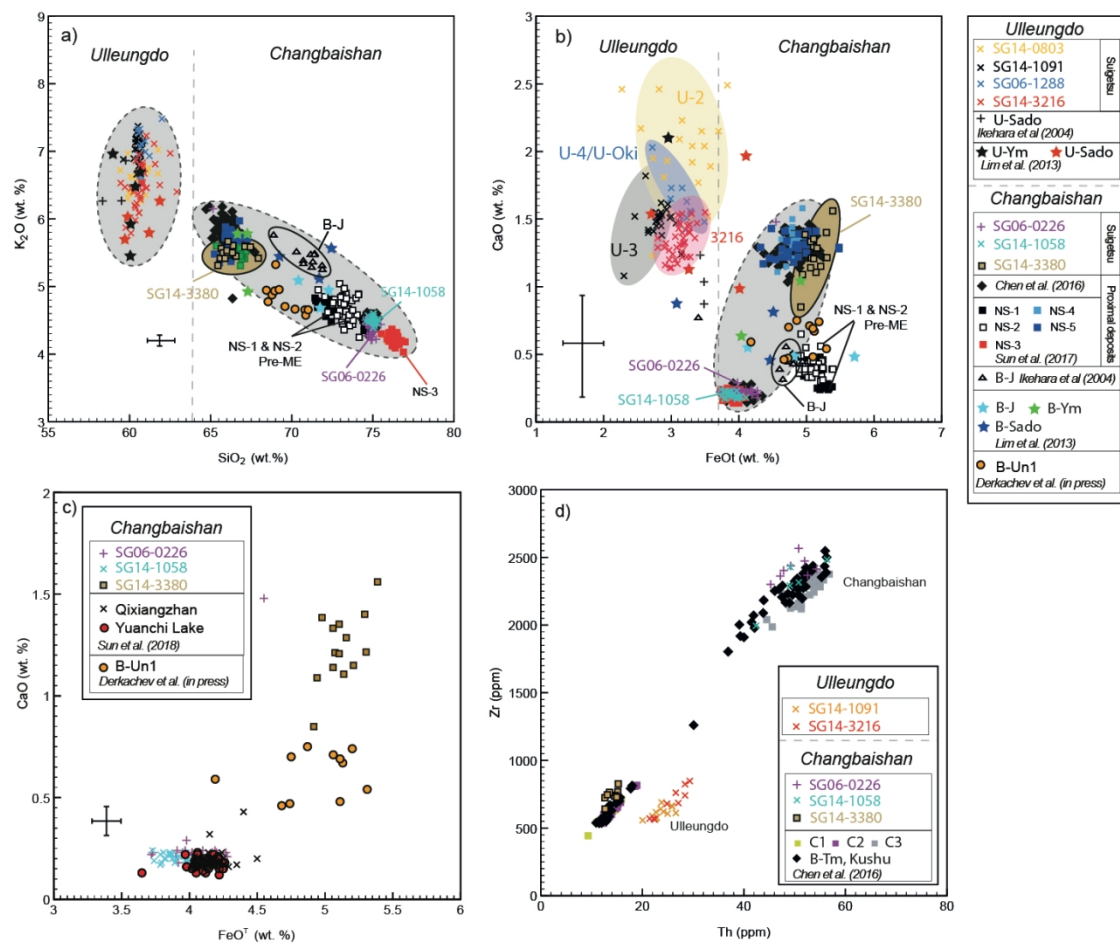


Figure 8. Glass shard major and trace element compositions of Ulleungdo (SG14-0803; SG14-1091; SG06-1288; SG14-3216) and Changbaishan (SG06-0226; SG14-1058; SG14-3380) tephra layers preserved in the Lake Suigetsu archive, compared to other proximal (Chen et al., 2016; Sun et al., 2017, 2018) and distal occurrences (Ikehara et al., 2004; Lim et al., 2013; Derkachev et al. (in press)). Error bars represent 2 x standard deviations of repeat analysis of the StHs6/80-G MPI-DING reference glass analyses, error bars for (d) are smaller than the data symbols.

Lim et al. (2013) also identified two equivalent cryptotephra layers in several other marine cores northeast of Ulleungdo (e.g., GH86-2-N, GH89-2-25, GH89-2-26 and GH89-2-28), which were stratigraphically positioned between the rhyolitic Aso-4 and AT tephra. These distal tephra layers were therein named the Ulleung-Yamato (U-Ym) and Ulleung-Sado-Oki (U-Sado), and are considered to be equivalent to SKP-I and SKP-II, respectively (Figure 7).

The Lake Suigetsu sediments verify that an ash fall event from Ulleungdo occurred at 40,332 – 39,816 IntCal13 yrs BP (95.4 % confidence interval). This 1 mm thick ash layer (SG14-3216; Figure 4) contains volcanic glass that compositionally overlaps the other Ulleungdo-derived tephra deposits preserved in the Suigetsu sequence (e.g. SG06-1288, SG14-1091), and other distal and proximal occurrences of the U-Oki tephra (Figure 5; Figure 8; Furuta et al., 1986; Nagahashi et al., 2004; Chun et al., 2007; Park et al., 2003, 2007).

Although grain-specific glass compositional datasets for the U-Ym tephra preserved in the Sea of Japan have not been published for comparison, the broad geochemical and chronological data and the stratigraphic position is consistent with SG14-3216, meaning this ash must also correlate to the same eruption of Ulleungdo. The Suigetsu-derived deposit age of 40,332 – 39,816 IntCal13 yrs BP (95.4 % confidence interval) provides the most precise eruption age, and this date can now be imported into other site-specific age models that contain this marker.

669 No other distal ash occurrences have been reported that are chronologically or
670 geochemically consistent with the ca. 19 ka eruption (proximal unit N-5; Kim et
671 al., 2014), suggesting that this eruption of Ulleungdo was probably not
672 widespread.

673

674 *5.1.2. Holocene Ulleungdo eruptions*

675

676 As previously outlined, the largest known Plinian eruption from Ulleungdo
677 generated the U-Oki tephra layer that is dated to 10,230 – 10,171 IntCal13 yrs
678 BP (95.4 % confidence interval; Smith et al., 2011, 2013). The U-Oki ash is
679 found in several high-resolution sedimentary records in Japan, including Lake
680 Biwa (BT-4; Nagahashi et al., 2004) and Lake Suigetsu (SG06-1288; Smith et
681 al., 2011) (Figure 7). This U-Oki tephra is the only distal tephra that has been
682 correlated to proximal deposits on Ulleungdo, and equates to the proximal U-4
683 unit of Shiihara et al. (2011).

684

685 Lake Suigetsu tephra layers SG14-1091 (ca. 8.4 ka) and SG14-0803 (ca. 5.7
686 ka) overlay the U-Oki tephra and are considered distal equivalents of proximal
687 deposits U-3 and U-2, respectively, due to their close agreement to the proximal
688 radiocarbon dates of soils between fall units (Okuno et al., 2010). Furthermore,
689 the K-Ah tephra is stratigraphically positioned between the U-3 (SG14-1091)
690 and U-2 (SG14-0803) deposits (Shiihara et al., 2011). Distal equivalents of the
691 U-3 eruption have been reported in the Sea of Japan (TRG1 sediment core;
692 Domitsu et al., 2002), Lake Biwa (Nagahashi et al., 2004), and close to
693 Hakusan volcano in central Honshu (Higashino et al., 2005). In comparison,

694 SG14-0803 is the only known distal equivalent of the U-2 tephra, indicating that
695 it was either a lower magnitude event or the eruption plume was dispersed in a
696 different direction.

697
698 The proximal deposits of the youngest U-1 eruption of Ulleungdo suggest it was
699 a small strombolian-type eruption with a lava dome extrusion (Kim et al., 2014).
700 Whole rock trace element data reported for this youngest event have a distinct
701 tephriphonolite composition (Brenna et al., 2014). Similarly, distal SG14-0433
702 glass compositions are distinct from those of other Ulleungdo derived tephras in
703 Suigetsu. Unfortunately, the lack of proximal glass chemistry for the U-1 unit
704 means that this correlation cannot be confirmed but it is likely that the SG14-
705 0433 layer at 2,737 – 2,620 IntCal13 yrs BP (95.4 % confidence interval)
706 correlates to the U-1 eruption.

708 5.2. Changbaishan eruption history

709
710 The newly identified Changbaishan-derived tephra layer outlined here, in
711 addition to the previously recognised layers, indicate that at least eight
712 explosive eruptions have produced widespread ash dispersals over the last 86
713 kyrs. These include the: ca. 85.8 ka B-Ym tephra (Lim et al., 2013); ca. 67.6 ka
714 B-Sado tephra (Lim et al., 2013); ca. 50.5 ka B-J tephra (Ikehara et al., 2014;
715 Lim et al., 2013); ca. 42.5 ka B-Sg-42 tephra (*this study*), ca. 38 ka B-Un1
716 tephra (Derkachev et al., in press), ca. 25 ka B-V tephra (Machida and Arai,
717 2003); ca. 8.1 ka B-Sg-08 tephra (McLean et al., 2018); and AD 946 B-Tm
718 tephra associated with the ME (McLean et al., 2016; Hakoziaki et al., 2017;

Oppenheimer et al., 2017). All the known distal ash deposits associated with eruptions at Changbaishan and possible correlations to proximal units on the volcano are summarised in Figure 7 and are discussed below.

5.2.1. Post 86 ka (Aso-4) Changbaishan eruptions

To date, at least four individual tephra layers originating from Changbaishan have been recognised in marine cores stratigraphically positioned between the Aso-4 and AT tephra layers (Figure 7). The two oldest, Baegdusan-Yamato Basin (B-Ym; ca. 85.8 ka) and Baegdusan-Sado-Oki (B-Sado; ca. 67.6 ka) tephra, have been identified as cryptotephra horizons in both the GH89-2-26 and GH89-2-28 marine cores (Figure 7; Lim et al., 2013). Lim et al. (2013) report that the B-Ym and B-Sado glass shards are trachytic in composition (Figure 8). More recently, Derkachev et al. (in press) also identify visible deposits in several marine cores across the Yamato and Pervenets Rise (e.g., cores Lv53-25, Lv53-20, Lv53-27, and Lv53-29) that they correlate to the B-Sado tephra. The constructed age models for these marine cores suggest an eruption age ca. 71 ka (Derkachev et al., in press).

The Baegdusan-Japan (B-J) tephra is found between Ulleungdo U-Ym and U-Sado tephra layers (Figure 7), and estimated to have been erupted at ca. 50 ka based on correlations with the regional-scale thinly laminated layer stratigraphy (Ikehara et al., 2004; Lim et al., 2013; Derkachev et al., in press). Ikehara et al. (2004) and Lim et al. (2013) report a homogenous rhyolitic composition for the B-J tephra, with ca. 71.2 wt. % SiO₂, ca. 12.0 wt. % Al₂O₃,

744 and total alkalis of 11.1 wt. % (Figure 8). It contrasts with the exclusively
 745 trachytic glass compositions of the older ca. 67.6 ka B-Sado tephra (Lim et al.,
 746 2013).
 747
 748 Derkachev et al. (in press) report a 5 mm thick volcanic ash layer in a sequence
 749 (Lv53-23 at 211 cm) from the Yamato Rise, about 270 km SE of Changbaishan,
 750 in the Sea of Japan. This deposit is therein named the Baegdusan-Unknown (B-
 751 Un1) tephra and represents another explosive event dated to around 38.3 ka.
 752 The glass chemistry of this layer is somewhat distinct, containing ca. 73.9 wt.
 753 %, ca. 13.5 wt. % Al_2O_3 , and total alkalis of 8.2 wt. %
 754
 755 The Lake Suigetsu sediments also provide evidence of another explosive
 756 eruption of Changbaishan chronologically occurring between the B-J and B-Un1
 757 event. A cryptotephra layer (SG14-3380) is found ca. 1.6 m below the U-Ym
 758 tephra (SG14-3216) and this depth corresponds to a date of 42,750 – 42,323
 759 IntCal13 yrs BP (95.4 % confidence interval). The glass compositions of SG14-
 760 3380 are exclusively trachytic and geochemically overlap with proximal units
 761 assigned to the late phase of the ME (e.g., NS-4 and NS-5 proximal deposits;
 762 Sun et al., 2017) (Figure 8) and other distal occurrences of the trachytic end
 763 member of the B-Tm ash (e.g., Okuno et al., 2011; Hughes et al., 2013; Sun et
 764 al., 2015; Chen et al., 2016). SG14-3380 does not geochemically overlap with
 765 the reported composition of the ca. 38 ka B-Un1 tephra reported in the Yamato
 766 Rise (Derkachev et al., in press), or the ca. 50.5 ka B-J tephra (Ikehara et al.,
 767 2004; Lim et al., 2013) clearly indicating that they represent separate eruptions
 768 of Changbaishan. Here, we name the Suigetsu distal ash of this Changbaishan

eruption (ca. 42 ka) as the Baegdusan-Suigetsu-42 (B-Sg-42) tephra, following the convention of naming proximally undefined distal deposits using the type-locality.

A post-AT distal tephra named the Baegdusan-Vladivostok (B-V) ash was found in the Primorye regions of Russia, and in the north-eastern part of the Japan Sea (Figure 1; Machida and Arai, 2003; Ikehara, 2003; Derkachev et al., in press). The eruption age is estimated to ca. 29 ka (Derkachev et al., in press).

5.2.2. Holocene Changbaishan eruptions

An eruption from Changbaishan was identified in Lake Suigetsu (SG14-1058) at 8,166 – 8,099 IntCal13 yrs BP (95.4 % confidence interval; McLean et al., 2018) and was the first known discovery of a large early Holocene eruption from this volcano. A visible patchy grey peralkaline tephra has since been identified in Lake Yuanchi, located ca. 30 km east of Changbaishan in China, which is dated to a similar age as the Suigetsu layer, 8,831 – 8,100 IntCal13 yrs BP (95.4 % confidence interval; Sun et al., 2018). The major element glass compositions of this Yuanchi tephra broadly overlap with those of SG14-1058 (Figure 8c), although some offsets, which are close to instrumental/analytical uncertainty, are observed. Sun et al. (2018) also suggest the Suigetsu SG14-1058 and Yuanchi tephra are distal deposits from the eruption that produced the Qixiangzhan comendite lava flow, but it is not known if there was an explosive phase associated with this eruption, and the stratigraphic relationship between the Qixiangzhan comendite and the explosive pre-ME fall deposits is not

known. Furthermore, the chronological uncertainty on $^{40}\text{Ar}/^{39}\text{Ar}$ ages for the Qixiangzhan comendite mean that it could be a separate eruption (e.g., Singer et al., 2014; Yang et al., 2014). When normalised to mantle concentrations, we find that SG14-1058 only shows a minor depletion in Nb, unlike SG06-0226 (B-Tm ash) and C-3 unit (Chen et al., 2016), which could help identify the proximal deposit. We suggest that the distal ash erupted from Changbaishan at ca. 8.1 ka (e.g., SG14-1508) is named Baegdusan-Suigetsu-08 (B-Sg-08).

No distal ash deposits have been identified that geochemically or chronologically overlap with the pre-ME proximal deposits of NS-4 and NS-5 that are dated to ca. 4 – 5 ka (Sun et al., 2017). Similarly, even in the high-resolution archives in northern Japan (e.g., Lake Kushu; Chen et al., 2019) there are no clear isochrons representing post-ME ash eruptions of Changbaishan.

6. Conclusions

Distal records can provide useful information on past eruption activity from volcanoes whose deposits are inaccessible for various reasons, e.g., burial or deposition into dynamic ocean environments. The new occurrences reported here and considered with other known distal alkali-rich ash units found in marine and lacustrine cores (spanning the last 86 kyrs) in the East Asian/Pacific region provide an improved eruption framework for intraplate volcanoes, Ulleungdo and Changbaishan. This framework shows that there are numerous

818 explosive eruptions responsible for distal ash fall events that are only cryptically
 819 recorded in the geological record.
 820
 821 Ulleungdo has erupted explosively at least five times over the last 86 kyrs (since
 822 the deposition of the Aso-4 tephra) and these are: the 60 – 61 ka U-Sado
 823 tephra (Lim et al., 2013); the ca. 40.1 ka U-Ym tephra (*this study*); the ca. 10 ka
 824 U-Oki/U-4 tephra (Smith et al., 2011; 2013); ca. 8.4 ka tephra (U-3; McLean et
 825 al., 2018); and the ca. 5.7 ka U-2 tephra (McLean et al., 2018). Furthermore, it
 826 is likely that a younger eruption from Ulleungdo occurred ca. 2.7 ka, but
 827 chemical analyses of proximal deposits are required to confirm the correlation.
 828 This age would be consistent with an eruption repose interval of <3 ka
 829 throughout the Holocene.
 830
 831 The new Changbaishan-derived tephra layers identified in the Suigetsu
 832 sediments indicate that at least eight explosive eruptions have produced
 833 significant ash dispersals over the last 86 kyrs which include the: ca. 85.8 ka B-
 834 Ym (Lim et al., 2013); ca. 70 ka B-Sado (Lim et al., 2013; Derkachev et al., in
 835 press); ca. 50.5 ka B-J tephra (Ikehara et al., 2014; Lim et al., 2013; Derkachev
 836 et al., in press); ca. 42.5 ka B-Sg-42 (*this study*), ca. 38 ka B-Un1 (Derkachev et
 837 al., in press), ca. 25 ka B-V (Machida and Arai, 2003); ca. 8.1 ka B-Sg-08
 838 (McLean et al., 2018); and AD 946 B-Tm tephra associated with the ME
 839 (Hakozaki et al., 2017; Oppenheimer et al., 2017). It is possible that additional
 840 ash fall events will be discovered in other distal records in the future, as there
 841 are some proximal units near Changbaishan (e.g., the compositionally distinct

NS-4 and NS-5 layers; Sun et al., 2017) that have not yet been correlated to distal markers.

Even though Lake Suigetsu is located ca. 500 km E of Ulleungdo and ca. 1000 km SSE of Changbaishan (i.e., not downwind of the current prevailing winds), tephra from these volcanoes is clearly preserved in the sediments. The eruptions responsible for the B-Sg-42 and B-Sg-08 distal tephra must have been large eruption events (i.e., greater than VEI 5-6), based on the shard concentrations preserved in Suigetsu (>18,000 shards per gram of dried sediment). Unfortunately, it is not possible to get better constraints on volume and magnitude of these events given that they have not yet been found as visible layers and have not been identified in multiple locations. The precise ages provided in this paper from the Lake Suigetsu chronology may help locate these deposits in other records, which may provide more information about the eruptions and the dispersal of the events. Critically, these tephra occurrences demonstrate that both Ulleungdo and Changbaishan have been more active than previously thought, and the ash plumes from these explosive eruptions were widespread.

Acknowledgements

The SG14 (formally 'Fukui-SG14') sediment coring campaign was funded by the Fukui Prefectural government, and the coring was conducted by the team of Seibushisui Co. Ltd. Japan, led by Mr. Atsumi Kitamura. KAKENHI grants by MEXT, Japan (15H021443 and 18H03744 to TN) as well as grants by Casio

Science Promotion Foundation were used to purchase laboratory equipment and consumables during the project. Trace element analysis was funded by the Japan Society for the Promotion of Science (JSPS) 2018 Summer Program. DM was funded by NERC (grant: NE/L002612/1) and part of the Environmental Research Doctoral Training Program at the University of Oxford. PGA and RAS were supported by Early Career Fellowships from the Leverhulme Trust (grant: ECF-2014-438 and ECF-2015-396). Geochemical bi-plots were generated using the RESET plot function (<https://c14.arch.ox.ac.uk>). We would like to thank the two anonymous reviewers for their feedback on an earlier version of the manuscript.

References

- Albert, P. G., Tomlinson, E. L., Smith, V. C., Di Roberto, A., Todman, A., Rosi, M., Marani, M., Muller, W. and Menzies, M. A. 2012. Marine-continental tephra correlations: volcanic glass geochemistry from the Marsili Basin and the Aeolian Islands, Southern Tyrrhenian Sea, Italy. *Journal of Volcanology and Geothermal Research*, 229: 74-94
- Albert, P. G., Tomlinson, E. L., Lane, C. S., Wulf, S., Smith, V. C., Coltelli, M., Keller, J., Castro, D. L., Manning, C. J., Müller, W. and Menzies, M. A. 2013. Late glacial explosive activity on Mount Etna: Implications for proximal–distal tephra correlations and the synchronisation of Mediterranean archives. *Journal of Volcanology and Geothermal Research*, 265: 9-26
- Albert, P. G., Smith, V. C., Suzuki, T., Tomlinson, E., Nakagawa, T., Yamada, K., McLean, D., Staff, R. A., Scholaut, G., Takemura, K., Nagahashi, Y., Kimura, I-P, SG06 Project Members. 2018. Constraints on the frequency and dispersal of explosive eruptions at Sambe and Daisen volcanoes (South-West

- 896 Japan Arc) from the distal Lake Suigetsu record (SG06 core). *Earth-Science*
897 *Reviews*, 185: 1004-1028
- 898
- 899 Albert, P. G., Smith, V. C., Suzuki, T., McLean, D., Tomlinson, E. L., Miyabuchi,
900 Y., Kitaba, I., Mark, D. F., Moriwaki, H., SG06 Project Members, Nakagawa, T.
901 2019. Geochemical characterisation of the widespread Japanese
902 tephrostratigraphic markers and correlations to the Lake Suigetsu sedimentary
903 archive (SG06 core). *Quaternary Geochronology*, 52: 103 - 131
- 904
- 905 Arai, F., Oba, T., Kitazato, H., Horibe, Y., Machida, H. 1981. Late Quaternary
906 tephrochronology and paleo-oceanography of the sediments of the Japan Sea.
907 *Quaternary Research (Daiyonki-kenkyu)* 20: 209–230 (in Japanese, with
908 English Abstract)
- 909
- 910 Blockley, S. P. E., Pyne-O'Donnell, S. D. F., Lowe, J. J., Matthews, I. P., Stone,
911 A., Pollard, A. M., Turney, C. S. M. and Molyneux, E. G. 2005. A new and less
912 destructive laboratory procedure for the physical separation of distal glass
913 tephra shards from sediments. *Quaternary Science Reviews*, 24: 1952-1960
- 914
- 915 Brenna, M., Price, R., Cronin, S. J., Smith, I. E., Sohn, Y. K., Kim, G. B. and
916 Maas, R. 2014. Final magma storage depth modulation of explosivity and
917 trachyte–phonolite genesis at an intraplate volcano: a case study from Ulleung
918 Island, South Korea. *Journal of Petrology*, 55: 709-747
- 919
- 920 Bronk Ramsey, C. 2008. Deposition models for chronological records.
921 *Quaternary Science Reviews*, 27: 42-60
- 922
- 923 Bronk Ramsey, C. 2017 OxCal Project, Version 4.3. Retrieved December 2017.
924 <https://c14.arch.ox.ac.uk/oxcal/OxCal.html> Retrieved June 2017
- 925
- 926 Bronk Ramsey, C., Staff, R. A., Bryant, C. L., Brock, F., Kitagawa, H., Van Der
927 Plicht, J., Schlögl, G., Marshall, M. H., Brauer, A., Lamb, H. F., Payne, R. L.,
928 Tarasov, P. E. Haraguchi, T., Gotanda, K., Yonenobu, H., Yokoyama, Y., Tada,

- 929 R. and Nakagawa, T. 2012. A complete terrestrial radiocarbon record for 11.2 to
930 52.8 kyr BP. *Science*, 338: 370-374
- 931
- 932 Cassidy, M., Watt, S. F., Palmer, M. R., Trofimovs, J., Symons, W., Maclachlan,
933 S. E. and Stinton, A. J. 2014. Construction of volcanic records from marine
934 sediment cores: A review and case study (Montserrat, West Indies). *Earth-
935 Science Reviews*, 138: 137-155
- 936
- 937 Chen, S. S., Lee, S. G., Lee, T. J., Lee, Y. S. and Liu, J. Q. 2018. Multi-stage
938 magmatic plumbing system of the volcano: A case study from Ulleung Island,
939 South Korea. *Lithos*. 314: 201-215
- 940
- 941 Chen, X. Y., Blockley, S. P., Tarasov, P. E., Xu, Y. G., McLean, D., Tomlinson,
942 E. L., Albert, P. G., Liu, J. Q., Müller, S., Wagner, M. and Menzies, M. A., 2016.
943 Clarifying the distal to proximal tephrochronology of the Millennium (B–Tm)
944 eruption, Changbaishan Volcano, northeast China. *Quaternary Geochronology*,
945 33: 61-75
- 946
- 947 Chen X. Y., McLean, D., Blockley, S., Tarasov, P., Xu. Y. G. and Menzies, M.
948 2019. Developing a Holocene tephrostratigraphy for northern Japan using the
949 sedimentary record from Lake Kushu, Rebun Island, *Quaternary Science
950 Reviews*, 215: 272-292
- 951
- 952 Chun, J. H., Han, S. J. and Cheong, D. K., 1997. Tephrostratigraphy in the
953 Ulleung Basin, East Sea: Late Pleistocene to Holocene. *Geosciences Journal*,
954 1: 154-166
- 955
- 956 Chun, J. H., Cheong, D., Ikehara, K. and Han, S. J. 2007. Age of the SKP-I and
957 SKP-II tephras from the southern East Sea/Japan Sea: implications for
958 interstadial events recorded in sediment from marine isotope stages 3 and 4.
959 *Palaeogeography, Palaeoclimatology, Palaeoecology*, 247: 100-114
- 960

- 961 Cui, Z. X., Wei, H. Q., Liu, R. X. 1995. Historical documentation research of
 962 eruptions of the Tianchi volcano, Changbaishan. In: Liu, R.X. (Ed.), *Volcanism
 963 and Human Environment. Seismology Press, Beijing, pp. 36-39 (In Chinese).*
 964
- 965 Derkachev, A.N., Utkin, I.V., Nikolaeva, N.A., Gorbarenko, S.A., Malakhova,
 966 G.I., Portnyagin, M.V., Sakhno, V.G., Shi, X. and Lv, H. in press. Tephra layers
 967 of large explosive eruptions of Baitoushan/Changbaishan Volcano in the Japan
 968 Sea sediments. *Quaternary International*.
 969 <https://doi.org/10.1016/j.quaint.2019.01.043>
 970
- 971 Domitsu, H., Shiihara, M., Torii, M., Tsukawaki, S. and Oda, M. 2002.
 972 Tephrostratigraphy of the piston cored sediment KT96-17 P-2 in the southern
 973 Japan Sea: the eruption age of Daisen-Kusadanihara Pumice (KsP). *Journal of
 974 the Geological Society of Japan*. 108: 545-556 (in Japanese with English
 975 abstract)
 976
- 977 Furuta, T., Fujioka, K. and Arai, F. 1986. Widespread submarine tephra around
 978 Japan—petrographic and chemical properties. *Marine Geology*, 72: 125-142
 979
- 980 Hakozaiki, M., Miyake, F., Nakamura, T., Kimura, K., Masuda, K. and Okuno, M.
 981 2017. Verification of the Annual Dating of the 10th Century Baitoushan Volcano
 982 Eruption Based on an AD 774–775 Radiocarbon Spike. *Radiocarbon*, 60: 1-8
 983
- 984 Higashino, T., Tsujimori T. and Itaya T. 2005. An alkaline tephra found at
 985 Midagahara, Mt. Hakusan. 32. *Annual Report Hakusan Nature Conservation
 986 Center*, 32: 1 –7
 987
- 988 Horn, S. and Schmincke, H. U. 2000. Volatile emission during the eruption of
 989 Baitoushan Volcano (China/North Korea) ca. 969 AD. *Bulletin of Volcanology*,
 990 61: 537-555
 991
- 992 Hughes, P. D. M., Mallon, G., Brown, A., Essex, H. J., Stanford, J. D., Hotes, S.
 993 2013. The impact of high tephra loading on late-Holocene carbon accumulation

2641
2642
2643 994 and vegetation succession in peatland communities. *Quaternary Science*
2644
2645 995 *Reviews*, 67: 160-175
2646 996
2647
2648 997 Iacovino, K., Ju-Song, K., Sisson, T., Lowenstern, J., Kuk-Hun, R., Jong-Nam,
2649 J., Kun-Ho, S., Song-Hwan, H., Oppenheimer, C., Hammond, J. O. and
2650 998 Donovan, A. 2016. Quantifying gas emissions from the “Millennium Eruption” of
2651 999 Paektu volcano, Democratic People’s Republic of Korea/China. *Science*
2652 1000 *Advances*, 2: 1600913
2653 1001
2654 1002
2655
2656 1003 Ikehara, K. 2003. Late Quaternary seasonal sea-ice history of the North-eastern
2657 1004 Japan Sea. *Journal of Oceanography*, 59: 585-593
2658 1005
2659 1006 Ikehara, K., Kikkawa, K., Chun, J. H. 2004. Origin and correlation of three
2660 1007 tephras that erupted during oxygen isotope stage 3 found in cores from the
2661 1008 Yamato Basin, central Japan Sea. *The Quaternary Research*. 43, 201–212 (in
2662 1009 Japanese with English abstract)
2663 1010
2664 1011 Ikehara, K., Ohkushi, K., Noda, A., Danhara, T. and Yamashita, T. 2013. A new
2665 1012 local marine reservoir correction for the last deglacial period in the Sanriku
2666 1013 region, northwestern North Pacific, based on radiocarbon dates from the
2667 1014 Towada-Hachinohe (To-H) tephra. *The Quaternary Research*. 52: 127-37
2668 1015
2669 1016 Im, J. H., Shim, S. H., Choo, C. O., Jang, Y. D. and Lee, J. S. 2012.
2670 1017 Volcanological and palaeoenvironmental implication of charcoals of the Nari
2671 1018 Formation in Nari Caldera, Ulleung Island, Korea. *Geosciences Journal*, 16:
2672 1019 105-114
2673 1020
2674 1021 Jochum, K. P., Stoll, B., Herwig, K., Willbold, M., Hofmann, A. W., Amini, M. *et*
2675 1022 *al.*, 2006. MPI-DING reference glasses for in situ microanalysis: New reference
2676 1023 values for element concentrations and isotope ratios. *Geochemistry,*
2677 1024 *Geophysics, Geosystems*, 7: 2
2678 1025
2679
2680
2681
2682
2683
2684
2685
2686
2687
2688
2689
2690
2691
2692
2693
2694
2695
2696
2697
2698
2699
2700

2701
2702
2703 1026 Kim, Y. K. 1985. Petrology of Ulreung Volcanic Island. *The Journal of the*
2704
2705 1027 *Japanese Association of Mineralogists, Petrologists and Economic Geologists,*
2706 1028 80: 292–303
2707
2708 1029
2709
2710 1030 Kim, K. H, Tanaka T, Nagao K, Jang, S. K. 1999. Nd and Sr isotopes and K- Ar
2711 1031 ages of the Ulreungdo alkali volcanic rocks in the East Sea, South Korea.
2712 1032 *Geochemical Journal*, 33: 317–341
2713
2714 1033
2715
2716 1034 Kim, G. B., Cronin, S. J., Yoon, W. S. and Sohn, Y. K. 2014. Post 19 ka BP
2717 1035 eruptive history of Ulleung Island, Korea, inferred from an intra-caldera
2718 1036 pyroclastic sequence. *Bulletin of Volcanology*, 76: 802
2719
2720
2721 1037
2722 1038 Kimura, J. I. and Chang, Q. 2012. Origin of the suppressed matrix effect for
2723 1039 improved analytical performance in determination of major and trace elements
2724 1040 in anhydrous silicate samples using 200 nm femtosecond laser ablation sector-
2725 1041 field inductively coupled plasma mass spectrometry, *Journal of Analytical*
2726 1042 *Atomic Spectrometry*, 27: 1549 – 1559
2727
2728
2729 1043
2730 1044 Kimura, J. I., Nagahashi, Y., Satoguchi, Y. and Chang, Q. 2015. Origins of felsic
2731 1045 magmas in Japanese subduction zone: Geochemical characterizations of
2732 1046 tephra from caldera-forming eruptions< 5 Ma. *Geochemistry, Geophysics,*
2733 1047 *Geosystems*, 16: 2147-2174
2734
2735 1048
2736
2737 1049 Kitagawa, H. and van der Plicht, H. 1998a. A 40,000-year varve chronology
2738 1050 from Lake Suigetsu, Japan: Extension of the C-14 calibration curve.
2739 1051 *Radiocarbon*, 40: 505-515
2740
2741
2742 1052
2743 1053 Kitagawa, H. and van der Plicht, H. 1998b. Atmospheric Radiocarbon
2744 1054 Calibration to 45,000 yr B.P.: Late Glacial Fluctuations and Cosmogenic Isotope
2745 1055 Production. *Science*, 279: 1187-1190
2746
2747
2748 1056
2749 1057 Kitagawa, H. and van der Plicht, J. 2000. Atmospheric radiocarbon calibration
2750 1058 beyond 11,900 cal BP from Lake Suigetsu laminated sediments. *Radiocarbon*,
2751 1059 42: 370-381
2752
2753
2754
2755
2756
2757
2758
2759
2760

2761
2762
2763 1060
2764
2765 1061 Le Bas, M. J., Le Maitre, R. W., Streckeisen, A. and Zanettin, B. 1986. A
2766 1062 chemical classification of volcanic rocks based on the total alkali-silica diagram.
2767 1063 *Journal of petrology*, 27: 745-750
2768
2769 1064
2770
2771 1065 Lim, C., Toyoda, K., Ikehara, K. and Peate, D.W. 2013. Late Quaternary
2772 1066 tephrostratigraphy of Baegdusan and Ulleung volcanoes using marine
2773 1067 sediments in the Japan Sea/East Sea. *Quaternary Research*, 80: 76-87
2774
2775 1068
2776
2777 1069 Lim, C., Kim, S. and Lee, C. 2014. Geochemical fingerprint of the primary
2778 1070 magma composition in the marine tephra originated from the Baegdusan and
2779 1071 Ulleung volcanoes. *Journal of Asian Earth Sciences*, 95: 266-273
2780
2781 1072
2782
2783 1073 Liu, R. X., Wei, H. Q., Li, J. T. 1998. The Latest Eruptions from Tianchi Volcano.
2784 1074 Changbaishan. *Science Press*, Beijing, p. 159 (In Chinese)
2785
2786 1075
2787
2788 1076 Machida, H. and Arai, F. 1983. Extensive ash falls in and around the Sea of
2789 1077 Japan from large late Quaternary eruptions. *Journal of Volcanology and*
2790 1078 *Geothermal Research*, 18: 151-164
2791
2792 1079
2793
2794 1080 Machida, H. and Arai, F. 2003. *Atlas of tephra in and around Japan*. Revised
2795 1081 ed. Tokyo University Press, Tokyo
2796
2797 1082
2798
2799 1083 Machida, H., Arai, F., Lee, B., Moriwaki, H. and Furuta, T. 1984. Late
2800 1084 Quaternary tephra in Ulleung-do Island, Korea. *Journal of Geography*
2801 1085 (*Chigaku-Zasshi*), 93: 1-14 (in Japanese with English abstract)
2802
2803 1086
2804
2805 1087 Machida, H., H. Moriwaki, and D. Zhao. 1990. The recent major eruption of
2806 1088 Changbai volcano and its environmental effects. *Geographical Reports of*
2807 1089 *Tokyo Metropolitan University*, 25: 1-20
2808
2809 1090
2810
2811 1091 Marshall, M., Schlögl, G., Nakagawa, T., Lamb, H., Brauer, A., Staff, R.,
2812 1092 Ramsey, C.B., Tarasov, P., Gotanda, K., Haraguchi, T. and Yokoyama, Y.
2813 1093 2012. A novel approach to varve counting using μ XRF and X-radiography in
2814
2815
2816
2817
2818
2819
2820

2821
2822
2823 1094 combination with thin-section microscopy, applied to the Late Glacial
2824
2825 1095 chronology from Lake Suigetsu, Japan. *Quaternary Geochronology*, 13: 70-80
2826
2827 1096
2828 1097 Martin-Jones, C. 2012. *Defining fractionation in LA-ICP-MS analysis of volcanic*
2829
2830 1098 *glass shards and its application to the correlation of tephra deposits from*
2831 1099 *Ulleungdo, Korea* (Doctoral dissertation, MPhil thesis, Aberystwyth University).
2832
2833 1100
2834 1101 McLean, D., Albert, P. G., Nakagawa, T., Staff, R. A., Suzuki, T. and Smith,
2835
2836 1102 V.C. 2016. Identification of the Changbaishan 'Millennium' (B-Tm) eruption
2837
2838 1103 deposit in the Lake Suigetsu (SG06) sedimentary archive, Japan:
2839 1104 Synchronisation of hemispheric-wide palaeoclimate archives. *Quaternary*
2840
2841 1105 *Science Reviews*, 150: 301-307
2842
2843 1106
2844 1107 McLean, D., Albert, P. G., Nakagawa, T., Suzuki, T., Staff, R. A., Yamada, K.,
2845
2846 1108 Kitaba, I., Haraguchi, T., Kitagawa, J., Members, S.P. and Smith, V. 2018.
2847 1109 Integrating the Holocene tephrostratigraphy for East Asia using a high-
2848
2849 1110 resolution cryptotephra study from Lake Suigetsu (SG14 core), central Japan.
2850 1111 *Quaternary Science Reviews*, 183: 36-58
2851
2852 1112
2853 1113 Nagahashi, Y., Yoshikawa, S., Miyakawa, C., Uchiyama, T. and Inouchi, Y.
2854
2855 1114 2004. Stratigraphy and chronology of widespread tephra layers during the past
2856
2857 1115 430 ky in the Kinki District and the Yatsugatake Mountains: major element
2858 1116 composition of the glass shards using EDS analysis. *The Quaternary Research*
2859
2860 1117 *(Daiyonki-Kenkyu)*, 43: 15-35 (in Japanese with English abstract)
2861
2862 1118
2863 1119 Nakagawa, T., Kitagawa, H., Yasuda, Y., Tarasov, P. E., Gotanda, K. and
2864
2865 1120 Sawai, Y. 2005. Pollen/event stratigraphy of the varved sediment of Lake
2866 1121 Suigetsu, central Japan from 15,701 to 10,217 SG kyr BP (Suigetsu varve years
2867
2868 1122 before present): description, interpretation, and correlation with other regions.
2869 1123 *Quaternary Science Reviews* 24: 1691–1701
2870
2871 1124
2872 1125 Nakagawa, T., Gotanda, K., Haraguchi, T., Danhara, T., Yonenobu, H., Brauer,
2873
2874 1126 A., Yokoyama, Y., Tada, R., Takemura, K., Staff, R. A., Payne, R., Bronk
2875
2876 1127 Ramsey, C., Bryant, C., Brock, F., Schlolaut, G., Marshall, M., Tarasov, P.,
2877
2878
2879
2880

2881
2882
2883 1128 Lamb, H. and Suigetsu 2006 Project Members. 2012. SG06, a perfectly
2884
2885 1129 continuous and varved sediment core from Lake Suigetsu, Japan: stratigraphy
2886
2887 1130 and potential for improving the radiocarbon calibration model and
2888
2889 1131 understanding of late Quaternary climate changes. *Quaternary Science*
2890 1132 *Reviews*, 36: 164-176
2891 1133
2892
2893 1134 Nakajima, T., Kikkawa, K., Ikehara, K., Katayama, H., Kikkawa, E., Joshima, M.,
2894
2895 1135 Seto, K. 1996. Marine sediments and late Quaternary stratigraphy in the
2896
2897 1136 southeastern part of the Japan Sea – Concerning the timing of dark layer
2898
2899 1137 deposition. *Journal of Geological Society of Japan*, 102: 125 – 138 (in
2900
2901 1138 Japanese with English abstract)
2902
2903 1139
2904
2905 1140 Newhall, C. G. and Self, S. 1982. The volcanic explosivity index (VEI) an
2906
2907 1141 estimate of explosive magnitude for historical volcanism. *Journal of Geophysical*
2908
2909 1142 *Research: Oceans*, 87: 1231-1238
2910
2911 1143
2912
2913 1144 Okuno, M., Shiihara, M., Torii, M., Nakamura, T., Kim, K. H., Domitsu, H.,
2914
2915 1145 Moriwaki, H. and Oda, M. 2010. AMS radiocarbon dating of Holocene tephra
2916
2917 1146 layers on Ulleung Island, South Korea. *Radiocarbon*, 52: 1465-1470
2918
2919 1147
2920
2921 1148 Okuno, M., Torii, M., Yamada, K., Shinozuka, Y., Danhara, T., Gotanda, K.,
2922
2923 1149 Yonenobu, H. and Yasuda, Y. 2011. Widespread tephras in sediments from
2924
2925 1150 lake Ichi-no-Megata in northern Japan: Their description, correlation and
2926
2927 1151 significance. *Quaternary International*, 246: 270-277
2928
2929 1152
2930
2931 1153 Oppenheimer, C., Wacker, L., Xu, J., Galván, J. D., Stoffel, M., Guillet, S.,
2932
2933 1154 Corona, C., Sigl, M., Di Cosmo, N., Hajdas, I. and Pan, B. 2017. Multi-proxy
2934
2935 1155 dating the ‘Millennium Eruption’ of Changbaishan to late 946 CE. *Quaternary*
2936
2937 1156 *Science Reviews*, 158: 164-171
2938
2939 1157
2940
2941 1158 Pan, B., de Silva, S.L., Xu, J., Chen, Z., Miggins, D.P. and Wei, H. 2017. The
2942
2943 1159 VEI-7 Millennium eruption, Changbaishan-Tianchi volcano, China/DPRK: New
2944
2945 1160 field, petrological, and chemical constraints on stratigraphy, volcanology, and

2941
2942
2943 1161 magma dynamics. *Journal of Volcanology and Geothermal Research*, 343: 45-
2944 1162 59
2945 1163
2946
2947 1164 Park, M. H., Kim, I. S. and Shin, J. B. 2003. Characteristics of the late
2948 1165 Quaternary tephra layers in the East/Japan Sea and their new occurrences in
2949 1166 western Ulleung Basin sediments. *Marine Geology*, 202: 135-142
2950
2951 1167
2952
2953 1168 Park, M. H., Kim, J. H. and Kil, Y. W. 2007. Identification of the Late Quaternary
2954 1169 tephra layers in the Ulleung Basin of the East Sea using geochemical and
2955 1170 statistical methods. *Marine Geology*, 244: 196-208
2956
2957 1171
2958
2959 1172 Ponomareva, V., Polyak, L., Portnyagin, M., Abbott, P. M., Zelenin, E.,
2960 1173 Vakhrameeva, P. and Garbe-Schönberg, D. 2018. Holocene tephra from the
2961 1174 Chukchi-Alaskan margin, Arctic Ocean: Implications for sediment
2962 1175 chronostratigraphy and volcanic history. *Quaternary Geochronology*, 45: 85-97
2963
2964 1176
2965
2966 1177 Reimer, P. J., Bard, E., Bayliss, A., Beck, J. W., Blackwell, P. G., Ramsey, C.
2967 1178 B., Buck, C. E., Cheng, H., Edwards, R. L., Friedrich, M. and Grootes, P.M.
2968 1179 2013. IntCal13 and Marine13 radiocarbon age calibration curves 0–50,000
2969 1180 years cal BP. *Radiocarbon*, 55: 1869-1887
2970
2971 1181
2972
2973 1182 Sawada, Y., Nakamura, T., Umeda, Y., Yoon, S. and Tokuoka. 1997. Drifting
2974 1183 pumice clasts derived from Ulleung Island in early Holocene sediments at Oda,
2975 1184 Shimane Prefecture, Southwestern Japan. *The Quaternary Research (Daiyonki-*
2976 1185 *Kenkyu)*, 36: 1 – 16 (in Japanese with English abstract)
2977
2978 1186
2979
2980 1187 Schlolaut, G., Marshall, M. H., Brauer, A., Nakagawa, T., Lamb, H. F., Staff, R.
2981 1188 A., Bronk Ramsey, C., Bryant, C. L., Brock, F., Kossler, A., Tarasov, P. E.,
2982 1189 Yokoyama, Y., Tada, R. and Haraguchi, T. 2012. An automated method for
2983 1190 varve interpolation and its application to the Late Glacial chronology from Lake
2984 1191 Suigetsu, Japan. *Quaternary Geochronology*. 13: 52-69
2985
2986 1192
2987
2988 1193 Shiihara, M., Torii, M., Okuno, M., Domitsu, H., Nakamura, T., Kim, K.,
2989 1194 Moriwaki, H. and Oda, M. 2011. Revised stratigraphy of Holocene tephras on
2990
2991
2992
2993
2994
2995
2996
2997
2998
2999
3000

- 1195 Ulleung Island, South Korea, and possible correlatives for the U-Oki tephra.
 1196 *Quaternary International* 246: 222-232
 1197
 1198 Singer, B. S., Jicha, B. R., He, H. and Zhu, R. 2014. Geomagnetic field
 1199 excursion recorded 17 ka at Tianchi volcano, China: New $^{40}\text{Ar}/^{39}\text{Ar}$ age and
 1200 significance. *Geophysical Research Letters*, 41: 2794–2802
 1201
 1202 Smith, V. C., Mark, D. F., Staff, R. A., Blockley, S. P. E., Bronk-Ramsey, C.,
 1203 Bryant, C. L., Nakagawa, T., Han, K. K., Weh, A., Takemura, K., Danhara, T.
 1204 and Suigetsu 2006 Project Members. 2011. Toward establishing precise Ar/Ar
 1205 chronologies for Late Pleistocene palaeoclimate archives: an example from the
 1206 Lake Suigetsu (Japan) sedimentary record, *Quaternary Science Reviews*, 30:
 1207 2845-2850
 1208
 1209 Smith, V. C., Staff, R. A., Blockley, S. P. E., Bronk Ramsey, C., Nakagawa, T.,
 1210 Mark, D. F., Takemura, K., Danhara, T. 2013. Identification and correlation of
 1211 visible tephras in the Lake Suigetsu SG06 sedimentary archive, Japan:
 1212 Chronostratigraphic markers for synchronising of east Asian/west Pacific Pacific
 1213 palaeoclimatic records for 150 ka, *Quaternary Science Reviews*, 61: 121-137
 1214
 1215 Staff, R. A., Bronk Ramsey, C., Bryant, C. L., Brock, F., Payne, R. L., Schlolaut,
 1216 G., Marshall, M. H., Brauer, A., Lamb, H. F., Tarasov, P., Yokoyama, Y.,
 1217 Haraguchi, T., Gotanda, K., Yonenobu, H., Nakagawa, T. and Suigetsu 2006
 1218 project members. 2011. New ^{14}C determinations from Lake Suigetsu, Japan:
 1219 12,000 to 0 cal. BP, *Radiocarbon*, 53: 511-528
 1220
 1221 Staff, R. A., Schlolaut, G., Ramsey, C. B., Brock, F., Bryant, C. L., Kitagawa, H.,
 1222 Van der Plicht, J., Marshall, M. H., Brauer, A., Lamb, H. F. and Payne, R. L.
 1223 2013a. Integration of the old and new Lake Suigetsu (Japan) terrestrial
 1224 radiocarbon calibration data sets. *Radiocarbon*, 55: 2049-2058
 1225
 1226 Staff, R. A., Nakagawa, T., Schlolaut, G., Marshall, M.H., Brauer, A., Lamb, H.
 1227 F., Bronk Ramsey, C., Bryant, C. L., Brock, F., Kitagawa, H. and Plicht, J.,

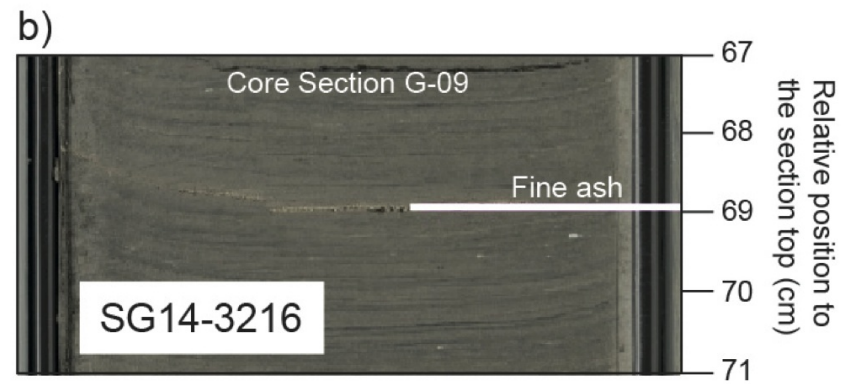
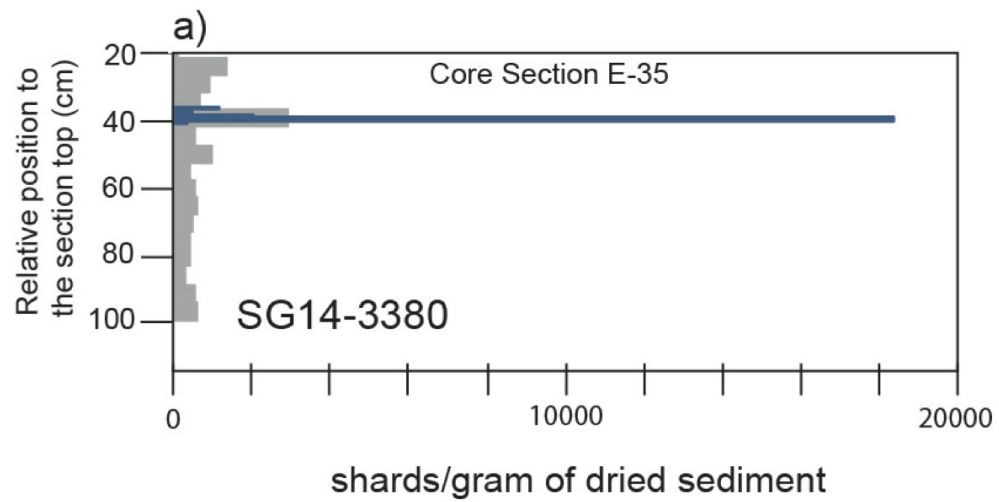
3061
3062
3063 1228 2013b. The multiple chronological techniques applied to the Lake Suigetsu
3064 SG06 sediment core, central Japan. *Boreas*, 42: 259-266
3065 1229
3066 1230
3067
3068 1231 Stone, R. 2010. Is China's riskiest volcano stirring or merely biding its time?
3069 1232 *Science*, 329: 498-499
3070
3071 1233
3072
3073 1234 Sun, S. S. and McDonough, W. F. 1989. Chemical and isotopic systematics of
3074 1235 oceanic basalts: implications for mantle composition and processes. *Geological*
3075 *Society, London, Special Publications*, 42: 313-345
3076 1236
3077 1237
3078
3079 1238 Sun, C., Plunkett, G., Liu, J., Zhao, H., Sigl, M., McConnell, J. R., Pilcher, J. R.,
3080 1239 Vinther, B., Steffensen, J. P. and Hall, V. 2014a. Ash from Changbaishan
3082 1240 Millennium eruption recorded in Greenland ice: Implications for determining the
3083 1241 eruptions timing and impact. *Geophysical Research Letters*, 41: 694-701
3084
3085 1242
3086
3087 1243 Sun, C., You, H., Liu, J., Li, X., Gao, J. and Chen, S. 2014b. Distribution,
3088 1244 geochemistry and age of the Millennium eruptives of Changbaishan volcano,
3090 1245 Northeast China—A review. *Frontiers of Earth Science*, 8: 216-230
3091
3092 1246
3093
3094 1247 Sun, C., You, H., He, H., Zhang, L., Gao, J., Guo, W., Chen, S., Mao, Q., Liu,
3095 1248 Q., Chu, G. and Liu, J., 2015. New evidence for the presence of Changbaishan
3096 1249 Millennium eruption ash in the Longgang volcanic field, Northeast China.
3098 1250 *Gondwana Research*, 28: 52-60
3099
3100 1251
3101
3102 1252 Sun, C., Liu, J., You, H. and Nemeth, K. 2017. Tephrostratigraphy of
3103 1253 Changbaishan volcano, northeast China, since the mid-Holocene. *Quaternary*
3104 1254 *Science Reviews*, 177: 104-119
3105
3106 1255
3107
3108 1256 Sun, C., Wang, L., Plunkett, G., You, H., Zhu, Z., Zhang, L., Zhang, B., Chu, G.
3109 1257 and Liu, J. 2018. Ash from the Changbaishan Qixiangzhan eruption: A new
3111 1258 early Holocene marker horizon across East Asia. *Journal of Geophysical*
3112 1259 *Research: Solid Earth*, 123: 6442-6450
3113
3114 1260
3115
3116
3117
3118
3119
3120

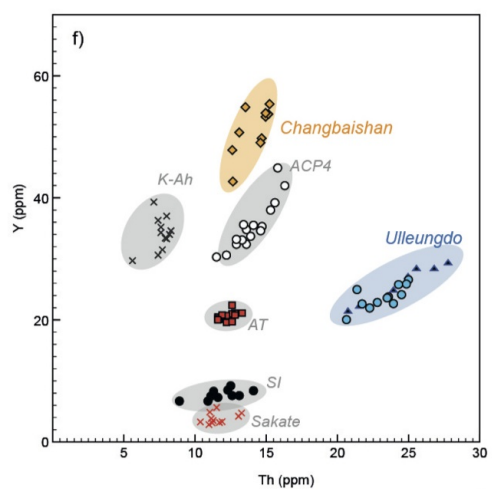
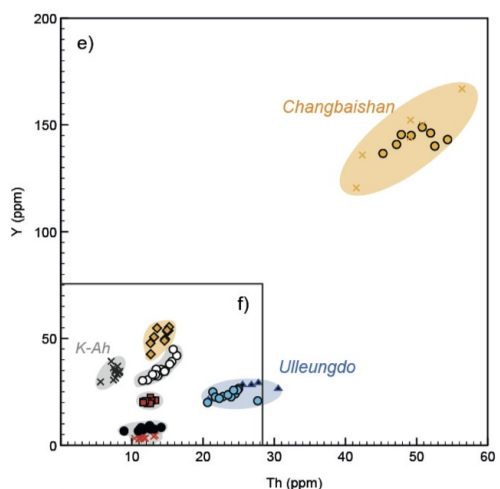
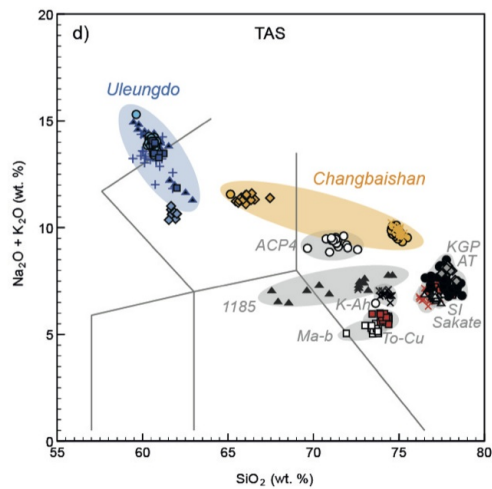
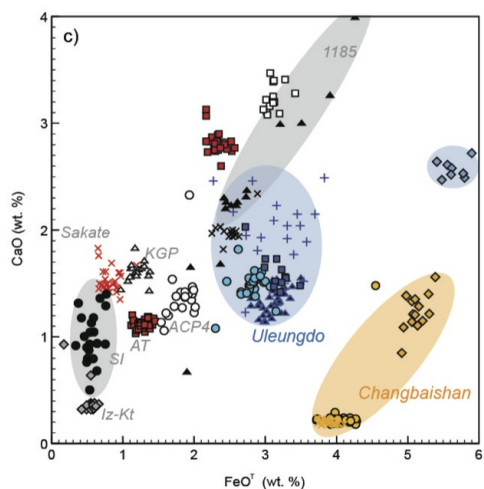
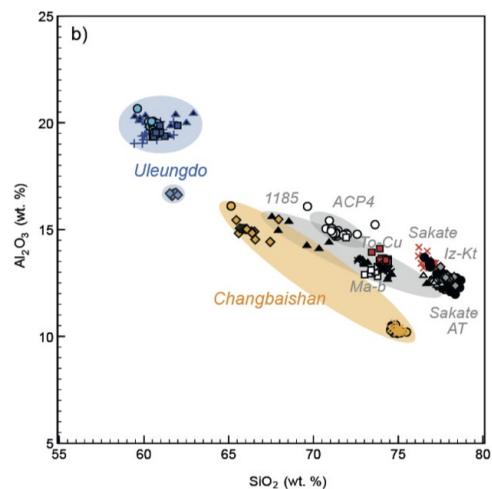
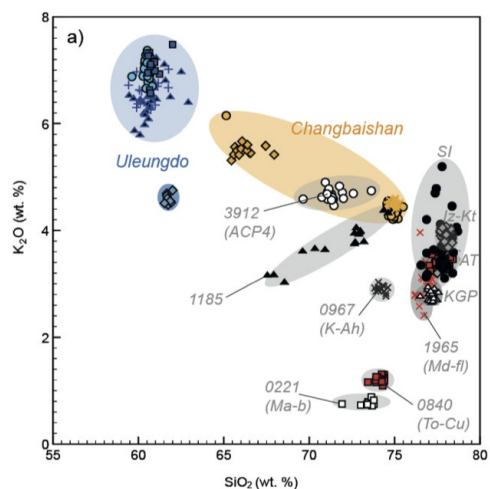
3121
3122
3123 1261 Tada, R. 1999. Late Quaternary paleoceanography of the Japan Sea. *The*
3124 *Quaternary Research (Daiyonki-Kenkyu)*, 38: 216-222
3125 1262
3126 1263
3127
3128 1264 Tada, R., Irino, T. and Koizumi, I. 1999. Land-ocean linkages over orbital and
3129 1265 millennial timescales recorded in Late Quaternary sediments of the Japan Sea.
3130 1266 *Paleoceanography*, 14: 236-247
3131
3132 1267
3133
3134 1268 Tomlinson, E. L., Albert, P. G., Wulf, S., Brown, R. J., Smith, V. C., Keller, J.,
3135 1269 Orsi, G., Bourne, A. J. and Menzies, M. A. 2014. Age and geochemistry of
3136 1270 tephra layers from Ischia, Italy: constraints from proximal-distal correlations with
3137 1271 Lago Grande di Monticchio. *Journal of Volcanology and Geothermal Research*,
3140 1272 287: 22-39
3141 1273
3142
3143 1274 Turney, C.S., 1998. Extraction of rhyolitic component of Vedde microtephra
3145 1275 from minerogenic lake sediments. *Journal of Paleolimnology*, 19: 199-206
3146 1276
3147
3148 1277 Tsukui, M., Saito, K. and Hayashi, K. 2006. Frequent and intensive eruptions in
3149 1278 the 9th century, Izu Islands, Japan: Revision of volcano-stratigraphy based on
3150 1279 tephras and historical document. *Bulletin of Volcanological Society of Japan*, 1:
3151 1280 327-338
3152 1281
3153
3154 1282 Wan, J. and Zheng, D. 2000. Several notable problems on dating of young
3155 1283 volcanic rocks by FT method-illustrated by dating of Changbaishan volcanic
3156 1284 rocks. *Seismology and Geology*, 22: 19-24 (In Chinese with English abstract)
3157 1285
3158
3159 1286 Wang, Y. J., Cheng, H., Edwards, R. L., An, Z. S., Wu, J. Y., Shen, C. C. and
3160 1287 Dorale, J. A. 2001. A high-resolution absolute-dated late Pleistocene monsoon
3161 1288 record from Hulu Cave, China. *Science*, 294: 2345-2348
3162 1289
3163
3164 1290 Wei, H., Wang, Y., Jin, J., Gao, L., Yun, S.H. and Jin, B. 2007. Timescale and
3165 1291 evolution of the intracontinental Tianchi volcanic shield and ignimbrite-forming
3166 1292 eruption, Changbaishan, Northeast China. *Lithos*, 96: 315-324
3167 1293
3168
3169
3170
3171
3172
3173
3174
3175
3176
3177
3178
3179
3180

- 1294 Wei, H., Liu, G. and Gill, J. 2013. Review of eruptive activity at Tianchi volcano,
1295 Changbaishan, northeast China: implications for possible future eruptions.
1296 *Bulletin of Volcanology*, 75: 706
1297
1298 Wulf, S., Kraml, M., Brauer, A., Keller, J. and Negendank, J.F. 2004.
1299 Tephrochronology of the 100 ka lacustrine sediment record of Lago Grande di
1300 Monticchio (southern Italy). *Quaternary International*, 122: 7-30
1301
1302 Xu, J., Liu, G., Wu, J., Ming, Y., Wang, Q., Cui, D., Shangguan, Z., Pan, B., Lin,
1303 X. and Liu, J. 2012. Recent unrest of Changbaishan volcano, northeast China:
1304 A precursor of a future eruption? *Geophysical Research Letters*, 39: 16
1305
1306 Yang, L., Wang, F., Feng, H., Wu, L. and Shi, W. 2014. $^{40}\text{Ar}/^{39}\text{Ar}$ geochronology
1307 of Holocene volcanic activity at Changbaishan, Northeast China. *Quaternary*
1308 *Geochronology*, 21: 106 – 114
1309
1310 Zou, H., Fan, Q., Zhang, H. 2010. Rapid development of the great millennium
1311 eruption of Changbaishan (Tianchi) volcano, China/North Korea: evidence from
1312 U-Th zircon dating. *Lithos*, 119: 289-296

id	name	email	password	status	created_at	updated_at
1	John Doe	john.doe@example.com	12345678	active	2023-01-01 10:00:00	2023-01-01 10:00:00
2	Jane Smith	jane.smith@example.com	87654321	active	2023-01-02 11:30:00	2023-01-02 11:30:00
3	Bob Johnson	bob.johnson@example.com	98765432	active	2023-01-03 09:15:00	2023-01-03 09:15:00
4	Alice Brown	alice.brown@example.com	56789012	active	2023-01-04 14:45:00	2023-01-04 14:45:00
5	Charlie Davis	charlie.davis@example.com	34567890	active	2023-01-05 16:20:00	2023-01-05 16:20:00
6	Diana Prince	diana.prince@example.com	23456789	active	2023-01-06 08:00:00	2023-01-06 08:00:00
7	Ethan Hunt	ethan.hunt@example.com	12345678	active	2023-01-07 12:30:00	2023-01-07 12:30:00
8	Fiona Glenanne	fiona.glenanne@example.com	09876543	active	2023-01-08 15:10:00	2023-01-08 15:10:00
9	Gavin Hastings	gavin.hastings@example.com	87654321	active	2023-01-09 10:45:00	2023-01-09 10:45:00
10	Helen Parr	helen.parr@example.com	76543210	active	2023-01-10 09:30:00	2023-01-10 09:30:00
11	Ivan Drago	ivan.drago@example.com	65432109	active	2023-01-11 13:00:00	2023-01-11 13:00:00
12	Jordan Peele	jordan.peele@example.com	54321098	active	2023-01-12 11:15:00	2023-01-12 11:15:00
13	Kyle Reese	kyle.reese@example.com	43210987	active	2023-01-13 14:00:00	2023-01-13 14:00:00
14	Liam Neeson	liam.neeson@example.com	32109876	active	2023-01-14 10:30:00	2023-01-14 10:30:00
15	Mel Gibson	mel.gibson@example.com	21098765	active	2023-01-15 09:00:00	2023-01-15 09:00:00
16	Nicole Kidman	nicole.kidman@example.com	10987654	active	2023-01-16 12:15:00	2023-01-16 12:15:00
17	Orlando Bloom	orlando.bloom@example.com	09876543	active	2023-01-17 15:45:00	2023-01-17 15:45:00
18	Penelope Cruz	penelope.cruz@example.com	98765432	active	2023-01-18 08:30:00	2023-01-18 08:30:00
19	Ryan Reynolds	ryan.reynolds@example.com	87654321	active	2023-01-19 11:00:00	2023-01-19 11:00:00
20	Sandra Bullock	sandra.bullock@example.com	76543210	active	2023-01-20 13:30:00	2023-01-20 13:30:00
21	Tom Cruise	tom.cruise@example.com	65432109	active	2023-01-21 10:15:00	2023-01-21 10:15:00
22	Uma Thurman	uma.thurman@example.com	54321098	active	2023-01-22 09:45:00	2023-01-22 09:45:00
23	Will Smith	will.smith@example.com	43210987	active	2023-01-23 12:00:00	2023-01-23 12:00:00
24	Xosha Roxx	xosha.roxx@example.com	32109876	active	2023-01-24 14:30:00	2023-01-24 14:30:00
25	Yasmine Paterlini	yasmine.paterlini@example.com	21098765	active	2023-01-25 11:45:00	2023-01-25 11:45:00
26	Zoe Lister-Jones	zoe.lister-jones@example.com	10987654	active	2023-01-26 15:00:00	2023-01-26 15:00:00
27	Adam Sandler	adam.sandler@example.com	09876543	active	2023-01-27 08:15:00	2023-01-27 08:15:00
28	Alfred Hitchcock	alfred.hitchcock@example.com	98765432	active	2023-01-28 10:45:00	2023-01-28 10:45:00
29	Barbra Streisand	barbra.streisand@example.com	87654321	active	2023-01-29 13:20:00	2023-01-29 13:20:00
30	Cary Elwes	cary.elwes@example.com	76543210	active	2023-01-30 09:00:00	2023-01-30 09:00:00
31	Dustin Diamond	dustin.diamond@example.com	65432109	active	2023-01-31 11:30:00	2023-01-31 11:30:00
32	Ewan McGregor	ewan.mcgregor@example.com	54321098	active	2023-02-01 14:00:00	2023-02-01 14:00:00
33	Faye Dunaway	faye.dunaway@example.com	43210987	active	2023-02-02 10:15:00	2023-02-02 10:15:00
34	Gary Oldman	gary.oldman@example.com	32109876	active	2023-02-03 09:45:00	2023-02-03 09:45:00
35	Halle Berry	halle.berry@example.com	21098765	active	2023-02-04 12:30:00	2023-02-04 12:30:00
36	Idina Menzel	idina.menzel@example.com	10987654	active	2023-02-05 15:00:00	2023-02-05 15:00:00
37	Jacob Tremblay	jacob.tremblay@example.com	09876543	active	2023-02-06 08:30:00	2023-02-06 08:30:00
38	Kate Winslet	kate.winslet@example.com	98765432	active	2023-02-07 11:00:00	2023-02-07 11:00:00
39	Liam Hemsworth	liam.hemsworth@example.com	87654321	active	2023-02-08 13:30:00	2023-02-08 13:30:00
40	Melanie Lynskey	melanie.lynskey@example.com	76543210	active	2023-02-09 10:15:00	2023-02-09 10:15:00
41	Nicole Scherzinger	nicole.scherzinger@example.com	65432109	active	2023-02-10 09:45:00	2023-02-10 09:45:00
42	Orlando Jones	orlando.jones@example.com	54321098	active	2023-02-11 12:00:00	2023-02-11 12:00:00
43	Penelope Wilton	penelope.wilton@example.com	43210987	active	2023-02-12 14:30:00	2023-02-12 14:30:00
44	Ryan Murphy	ryan.murphy@example.com	32109876	active	2023-02-13 11:45:00	2023-02-13 11:45:00
45	Sandra Oh	sandra.oh@example.com	21098765	active	2023-02-14 15:00:00	2023-02-14 15:00:00
46	Tom Hanks	tom.hanks@example.com	10987654	active	2023-02-15 08:15:00	2023-02-15 08:15:00
47	Uma Thurman	uma.thurman@example.com	09876543	active	2023-02-16 10:45:00	2023-02-16 10:45:00
48	Will Smith	will.smith@example.com	98765432	active	2023-02-17 13:20:00	2023-02-17 13:20:00
49	Xosha Roxx	xosha.roxx@example.com	87654321	active	2023-02-18 15:00:00	2023-02-18 15:00:00
50	Yasmine Paterlini	yasmine.paterlini@example.com	76543210	active	2023-02-19 08:30:00	2023-02-19 08:30:00
51	Zoe Lister-Jones	zoe.lister-jones@example.com	65432109	active	2023-02-20 11:00:00	2023-02-20 11:00:00
52	Adam Sandler	adam.sandler@example.com	54321098	active	2023-02-21 13:30:00	2023-02-21 13:30:00
53	Alfred Hitchcock	alfred.hitchcock@example.com	43210987	active	2023-02-22 10:15:00	2023-02-22 10:15:00
54	Barbra Streisand	barbra.streisand@example.com	32109876	active	2023-02-23 09:45:00	2023-02-23 09:45:00
55	Cary Elwes	cary.elwes@example.com	21098765	active	2023-02-24 12:30:00	2023-02-24 12:30:00
56	Dustin Diamond	dustin.diamond@example.com	10987654	active	2023-02-25 15:00:00	2023-02-25 15:00:00
57	Ewan McGregor	ewan.mcgregor@example.com	09876543	active	2023-02-26 08:30:00	2023-02-26 08:30:00
58	Faye Dunaway	faye.dunaway@example.com	98765432	active	2023-02-27 11:00:00	2023-02-27 11:00:00
59	Gary Oldman	gary.oldman@example.com	87654321	active	2023-02-28 13:30:00	2023-02-28 13:30:00
60	Halle Berry	halle.berry@example.com	76543210	active	2023-02-29 10:15:00	2023-02-29 10:15:00
61	Idina Menzel	idina.menzel@example.com	65432109	active	2023-03-01 09:45:00	2023-03-01 09:45:00
62	Jacob Tremblay	jacob.tremblay@example.com	54321098	active	2023-03-02 12:00:00	2023-03-02 12:00:00
63	Kate Winslet	kate.winslet@example.com	43210987	active	2023-03-03 14:30:00	2023-03-03 14:30:00
64	Liam Hemsworth	liam.hemsworth@example.com	32109876	active	2023-03-04 11:45:00	2023-03-04 11:45:00
65	Melanie Lynskey	melanie.lynskey@example.com	21098765	active	2023-03-05 15:00:00	2023-03-05 15:00:00
66	Nicole Scherzinger	nicole.scherzinger@example.com	10987654	active	2023-03-06 08:30:00	2023-03-06 08:30:00
67	Orlando Jones	orlando.jones@example.com	09876543	active	2023-03-07 10:45:00	2023-03-07 10:45:00
68	Penelope Wilton	penelope.wilton@example.com	98765432	active	2023-03-08 13:20:00	2023-03-08 13:20:00
69	Ryan Murphy	ryan.murphy@example.com	87654321	active	2023-03-09 15:00:00	2023-03-09 15:00:00
70	Sandra Oh	sandra.oh@example.com	76543210	active	2023-03-10 08:30:00	2023-03-10 08:30:00
71	Tom Hanks	tom.hanks@example.com	65432109	active	2023-03-11 11:00:00	2023-03-11 11:00:00
72	Uma Thurman	uma.thurman@example.com	54321098	active	2023-03-12 13:30:00	2023-03-12 13:30:00
73	Will Smith	will.smith@example.com	43210987	active	2023-03-13 10:15:00	2023-03-13 10:15:00
74	Xosha Roxx	xosha.roxx@example.com	32109876	active	2023-03-14 09:45:00	2023-03-14 09:45:00
75	Yasmine Paterlini	yasmine.paterlini@example.com	21098765	active	2023-03-15 12:00:00	2023-03-15 12:00:00
76	Zoe Lister-Jones	zoe.lister-jones@example.com	10987654	active	2023-03-16 14:30:00	2023-03-16 14:30:00
77	Adam Sandler	adam.sandler@example.com	09876543	active	2023-03-17 11:45:00	2023-03-17 11:45:00
78	Alfred Hitchcock	alfred.hitchcock@example.com	98765432	active	2023-03-18 15:00:00	2023-03-18 15:00:00
79	Barbra Streisand	barbra.streisand@example.com	87654321	active	2023-03-19 08:30:00	2023-03-19 08:30:00
80	Cary Elwes	cary.elwes@example.com	76543210	active	2023-03-20 11:00:00	2023-03-20 11:00:00
81	Dustin Diamond	dustin.diamond@example.com	65432109	active	2023-03-21 13:30:00	2023-03-21 13:30:00
82	Ewan McGregor	ewan.mcgregor@example.com	54321098	active	2023-03-22 10:15:00	2023-03-22 10:15:00
83	Faye Dunaway	faye.dunaway@example.com	43210987	active	2023-03-23 09:45:00	2023-03-23 09:45:00
84	Gary Oldman	gary.oldman@example.com	32109876	active	2023-03-24 12:00:00	2023-03-24 12:00:00
85	Halle Berry	halle.berry@example.com	21098765	active	2023-03-25 14:30:00	2023-03-25 14:30:00
86	Idina Menzel	idina.menzel@example.com	10987654	active	2023-03-26 11:45:00	2023-03-26 11:45:00
87	Jacob Tremblay	jacob.tremblay@example.com	09876543	active	2023-03-27 15:00:00	2023-03-27 15:00:00
88	Kate Winslet	kate.winslet@example.com	98765432	active	2023-03-28 08:30:00	2023-03-28 08:30:00
89	Liam Hemsworth	liam.hemsworth@example.com	87654321	active	2023-03-29 11:00:00	2023-03-29 11:00:00
90	Melanie Lynskey	melanie.lynskey@example.com	76543210	active	2023-03-30 13:30:00	2023-03-30 13:30:00
91	Nicole Scherzinger	nicole.scherzinger@example.com	65432109	active	2023-03-31 10:15:00	2023-03-31 10:15:00
92	Orlando Jones	orlando.jones@example.com	54321098	active	2023-04-01 09:45:00	2023-04-01 09:45:00
93	Penelope Wilton	penelope.wilton@example.com	43210987	active	2023-04-02 12:00:00	2023-04-02 12:00:00
94	Ryan Murphy	ryan.murphy@example.com	32109876	active	2023-04-03 14:30:00	2023-04-03 14:30:00
95	Sandra Oh	sandra.oh@example.com	21098765	active	2023-04-04 11:45:00	2023-04-04 11:45:00
96	Tom Hanks	tom.hanks@example.com	10987654	active	2023-04-05 15:00:00	2023-04-05 15:00:00
97	Uma Thurman	uma.thurman@example.com	09876543	active	2023-04-06 08:30:00	2023-04-06 08:30:00
98	Will Smith	will.smith@example.com	98765432	active	2023-04-07 11:00:00	2023-04-07 11:00:00
99	Xosha Roxx	xosha.roxx@example.com	87654321	active	2023-04-08 13:30:00	2023-04-08 13:30:00
100	Yasmine Paterlini	yasmine.paterlini@example.com	76543210	active	2023-04-09 10:15:00	2023-04-09 10:15:00

[illegible]





Changbaishan

- SG06-0226 (B-Tm)
- × SG14-1058 (B-Sg-08)
- ◆ SG14-3380 (B-Sg-42)

Ulleungdo

- ◆ SG14-0433 (U-1?)
- + SG14-0803 (U-2)
- SG14-1091 (U-3)
- SG06-1288 (U-4/U-Oki)
- ▲ SG14-3216 (U-Ym)

Key widespread Japanese tephras

- SG14-0221 (M-ab)
- ◆ SG14-0239 (Iz-Kt)
- △ SG14-0490 (KGP)
- SG14-0840 (To-Cu)
- × SG14-0977 (K-Ah)
- ▲ SG14-1185
- × SG06-1965 (Mdfl)
- SG06-2650 (AT)
- SG06-3668 (SI)
- SG06-3912 (ACP4)

1. The first part of the document discusses the importance of maintaining accurate records of all transactions and activities. It emphasizes the need for transparency and accountability in financial reporting.

2. The second part of the document outlines the various methods and techniques used to collect and analyze data. It includes a detailed description of the experimental procedures and the statistical analysis performed.

3. The third part of the document presents the results of the study, including a comparison of the different methods and techniques used. It also discusses the limitations of the study and the need for further research.

4. The fourth part of the document provides a conclusion and a summary of the findings. It also includes a list of references and a bibliography.

5. The fifth part of the document contains a list of figures and tables, which are used to illustrate the results of the study. It also includes a list of appendices and a bibliography.

6. The sixth part of the document contains a list of references and a bibliography, which are used to provide context and support for the findings of the study.

7. The seventh part of the document contains a list of references and a bibliography, which are used to provide context and support for the findings of the study.

8. The eighth part of the document contains a list of references and a bibliography, which are used to provide context and support for the findings of the study.

9. The ninth part of the document contains a list of references and a bibliography, which are used to provide context and support for the findings of the study.

10. The tenth part of the document contains a list of references and a bibliography, which are used to provide context and support for the findings of the study.

11. The eleventh part of the document contains a list of references and a bibliography, which are used to provide context and support for the findings of the study.

12. The twelfth part of the document contains a list of references and a bibliography, which are used to provide context and support for the findings of the study.

13. The thirteenth part of the document contains a list of references and a bibliography, which are used to provide context and support for the findings of the study.

14. The fourteenth part of the document contains a list of references and a bibliography, which are used to provide context and support for the findings of the study.

15. The fifteenth part of the document contains a list of references and a bibliography, which are used to provide context and support for the findings of the study.

16. The sixteenth part of the document contains a list of references and a bibliography, which are used to provide context and support for the findings of the study.

17. The seventeenth part of the document contains a list of references and a bibliography, which are used to provide context and support for the findings of the study.

18. The eighteenth part of the document contains a list of references and a bibliography, which are used to provide context and support for the findings of the study.

19. The nineteenth part of the document contains a list of references and a bibliography, which are used to provide context and support for the findings of the study.

20. The twentieth part of the document contains a list of references and a bibliography, which are used to provide context and support for the findings of the study.

21. The twenty-first part of the document contains a list of references and a bibliography, which are used to provide context and support for the findings of the study.

22. The twenty-second part of the document contains a list of references and a bibliography, which are used to provide context and support for the findings of the study.

23. The twenty-third part of the document contains a list of references and a bibliography, which are used to provide context and support for the findings of the study.

24. The twenty-fourth part of the document contains a list of references and a bibliography, which are used to provide context and support for the findings of the study.

25. The twenty-fifth part of the document contains a list of references and a bibliography, which are used to provide context and support for the findings of the study.

26. The twenty-sixth part of the document contains a list of references and a bibliography, which are used to provide context and support for the findings of the study.

27. The twenty-seventh part of the document contains a list of references and a bibliography, which are used to provide context and support for the findings of the study.

28. The twenty-eighth part of the document contains a list of references and a bibliography, which are used to provide context and support for the findings of the study.

29. The twenty-ninth part of the document contains a list of references and a bibliography, which are used to provide context and support for the findings of the study.

30. The thirtieth part of the document contains a list of references and a bibliography, which are used to provide context and support for the findings of the study.

31. The thirty-first part of the document contains a list of references and a bibliography, which are used to provide context and support for the findings of the study.

32. The thirty-second part of the document contains a list of references and a bibliography, which are used to provide context and support for the findings of the study.

33. The thirty-third part of the document contains a list of references and a bibliography, which are used to provide context and support for the findings of the study.

34. The thirty-fourth part of the document contains a list of references and a bibliography, which are used to provide context and support for the findings of the study.

35. The thirty-fifth part of the document contains a list of references and a bibliography, which are used to provide context and support for the findings of the study.

36. The thirty-sixth part of the document contains a list of references and a bibliography, which are used to provide context and support for the findings of the study.

1

2

3

4

5

6

7

8

9

10

11

12

13

14

15

16

17

18

19

20

21

22

23

24

25

26

27

28

29

30

31

32

33

34

35

36

37

38

39

40

41

42

43

44

45

46

47

48

49

50

51

52

53

54

55

56

57

58

59

60

61

62

63

64

65

66

67

68

69

70

71

72

73

74

75

76

77

78

79

80

81

82

83

84

85

86

87

88

89

90

91

92

93

94

95

96

97

98

99

100

101

102

103

104

105

106

107

108

109

110

111

112

113

114

115

116

117

118

119

120

121

122

123

124

125

126

127

128

129

130

131

132

133

134

135

136

137

138

139

140

141

142

143

144

145

146

147

148

149

150

151

152

153

154

155

156

157

158

159

160

